JOURNAL OF THE EXPERIMENTAL ANALYSIS OF BEHAVIOR 1993, 60, 361-385 NUMBER 2 (SEPTEMBER)

DRL INTERRESPONSE-TIME DISTRIBUTIONS: QUANTIFICATION BY PEAK DEVIATION ANALYSIS

JERRY B. RICHARDS, KAREN E. SABOL, AND LEWIS S. SEIDEN

THE UNIVERSITY OF CHICAGO

Peak deviation analysis is a quantitative technique for characterizing interresponse-time distributions that result from training on differential-reinforcement-of-low-rate schedules of reinforcement. It compares each rat's obtained interresponse-time distribution to the corresponding negative exponential distribution that would have occurred if the rat had emitted the same number of responses randomly in time, at the same rate. The comparison of the obtained distributions with corresponding negative exponential distributions provides the basis for computing three standardized metrics (burst ratio, peak location, and peak area) that quantitatively characterize the profile of the obtained interresponse-time distributions. In Experiment 1 peak deviation analysis quantitatively described the difference between the interresponse-time distributions of rats trained on variable-interval 300-s and differential-reinforcement-of-low-rate 72-s schedules of reinforcement. In Experiment 2 peak deviation analysis differentiated between the effects of the psychomotor stimulant *d*-amphetamine, the anxiolytic compound chlordiazepoxide, and the antidepressant desipramine. The results suggest that peak deviation analysis of interresponse-time distributions may provide a useful behavioral assay system for characterizing the effects of drugs.

Key words: interresponse time, differential-reinforcement-of-low-rate schedule, variable-interval schedule, *d*-amphetamine, chlordiazepoxide, desipramine, lever press, rats

Response rate has proven to be a useful way to measure behavioral output. Interresponse-time (IRT) distributions provide an additional way to characterize the temporal occurrence of behavior. However, no generally accepted way of quantitatively characterizing IRT distributions has been developed. Typically, IRT distributions have been compared graphically using relative frequency histograms or the IRTs per opportunity plot developed by Anger (1956). Because of the reliance upon graphical techniques, the comparison of IRT distributions is more difficult and less exact than the comparison of response rates.

This paper describes a quantitative approach to analyzing IRT distributions called peak deviation analysis. We developed peak deviation analysis specifically to handle IRT distributions that result from training on differential-reinforcement-of-low-rate (DRL) schedules of reinforcement. The results of peak deviation analysis are summarized numerically by metrics. The primary reason for developing peak deviation analysis was to provide a method for quantitatively describing important characteristics of DRL IRT distributions so that IRT analysis would perhaps approximate the usefulness of response rate in describing behavioral output. With quantitative metrics, IRT distributions can be compared in a manner similar to the way that response rates are compared. As quantitative dependent variables, the metrics provided by peak deviation analysis can be analyzed in ways that IRT plots cannot be (i.e., dose-effect curves and statistical inference). Another reason for developing peak deviation analysis is that much information about an organism's response output is ignored when only response rate or the molar patterns of behavior depicted in cumulative records are considered. As others (Weiss, 1970; Williams, 1968) have pointed out, IRT distributions provide a description of the structure of response rate.

One application in which IRT analysis provides important information is the assessment of drug effects on behavior. For example, in this laboratory, the DRL 72-s schedule of reinforcement has been developed as a behavioral screen for antidepressant drugs (Marek, Li, & Seiden, 1989; McGuire & Seiden, 1980; O'Donnell & Seiden, 1982; Seiden, Dahms, & Shaughnessy, 1985; Seiden & O'Donnell, 1985). The primary quantitative measure for this screen has been the number of reinforce-

This work was supported by U.S. Public Health Service Grant MH-11191 and by Research Scientist Award RSA MH-10562 to L. S. Seiden. We thank David Jolly for helpful comments and criticisms of this paper and Matthew Baggott for technical assistance. Reprints may be obtained from Jerry B. Richards, Department of Pharmacological and Physiological Sciences, University of Chicago, 947 East 58th St., Chicago, Illinois 60637.

ments earned on a DRL 72-s schedule. Antidepressant compounds increase the rate of reinforcement. Recently, however, work from this laboratory has indicated that increases in reinforcement rate could be accompanied by very different effects on the IRT distributions. Richards and Seiden (1991) compared the effects of the antidepressant drug desipramine and the serotonin 1A agonist gepirone on the DRL 72-s schedule. Both drugs decreased response rate and increased reinforcement rate. The effects of desipramine and gepirone on the IRT distribution, however, were markedly different. Desipramine shifted the peak toward longer durations without disrupting the IRT distribution (i.e., the size or area of the IRT distribution peak was not decreased). In contrast, gepirone did not affect the peak location and disrupted the IRT distribution (i.e., the size or area of the IRT distribution peak was decreased). These results demonstrate the potential of IRT analysis to discriminate between the behavioral effects of two compounds that have similar effects on response and reinforcement rate.

The approach to IRT analysis used by Richards and Seiden (1991) was based upon the principle that if an organism emitted responses randomly in time at a constant overall rate, the resulting IRT distribution would be described by a negative exponential function. A number of investigators in operant conditioning and behavioral ethology have used this fact to help analyze behavioral output (Blough, 1963, 1966; Duncan, Horne, Hughes, & Wood-Gush, 1970; Fagen & Young, 1978; Mueller, 1950; Norman, 1966; Revusky, 1962; Sidman, 1954; Slater & Lester, 1980). Mueller (1950) and Sidman (1954) were the first to use the negative exponential function to analyze operant IRT distributions. Mueller showed that the IRT distribution of a rat responding on a fixed-interval schedule of reinforcement (early in training) closely followed a negative exponential distribution. Sidman reported that cats and rats responding on shock-avoidance schedules frequently had IRT distributions that were well described by a negative exponential. Both Mueller and Sidman provided only graphical evidence that the obtained and exponential IRT distributions were similar.

The IRT analysis described by Richards and Seiden (1991) also compared the obtained IRT distribution of an individual rat to a corresponding negative exponential (CNE) distribution. The CNE distribution predicted the appearance of the obtained IRT distribution if the rat had randomly emitted the same number of responses over the same time interval. The CNE distribution was defined as a negative exponential distribution that had the same mean IRT duration as the obtained IRT distribution. The word *corresponding* was used to describe this negative exponential distribution because it indicates that for each rat's obtained IRT distribution, a CNE random distribution was determined. Importantly, because the CNE is determined by the mean of the obtained IRT distribution, the predictions of the CNE adjust as the mean of the obtained IRT distribution for each rat changes. This adjustment provides a baseline from which deviations of the obtained IRT distribution from the CNE can be systematically evaluated. Adjustment of the CNE insures that deviations from the CNE are equivalent for obtained distributions with different mean IRT durations.

The quantitative IRT analysis presented in this paper (peak deviation analysis) also relies on comparing the obtained IRT distribution with the CNE distribution. However, it differs from previous analyses, including that of Richards and Seiden (1991), in that it develops three specific metrics for quantifying DRL IRT distributions with respect to the CNE. The IRT distribution is divided into pause and burst components. Two metrics, peak area (PkA) and peak location (PkL), describe the pause component and a third metric, burst ratio (BR), describes the burst component. PkL and PkA are determined by using a peak-finding algorithm that locates the largest deviation (peak) of the obtained pause distribution above the CNE. PkL is the median IRT duration of the peak, and PkA is the proportion of IRT durations in the peak not accounted for by the CNE (area above the negative exponential). BR is the total number of obtained IRT durations in the burst component divided by the total number of IRT durations predicted to occur in the burst component by the CNE. The IRT histogram plots in this paper are presented in order to provide qualitative support for our analysis and to increase understanding of exactly what the peak deviation

analysis metrics are measuring. Importantly, the IRT histogram plots are not the end point of peak deviation analysis. The end results of peak deviation analysis are the three metrics: BR, PkA, and PkL.

The purposes of this paper are (a) to provide a complete description of peak deviation analysis in the General Method section below and (b) to present the results of two experiments that provide empirical evidence for the usefulness of peak deviation analysis. In Experiment 1, rats were first trained on a variable-interval (VI) 300-s schedule and were then trained on a DRL 72-s schedule. VI 300-s training produced IRT distributions that were similar to the CNE with small PkL and PkA values. Training on the DRL 72-s schedule caused the pause IRT distributions to diverge systematically from the CNE, resulting in increases in the values of PkL and PkA. In Experiment 2, the effects of the psychomotor stimulant *d*-amphetamine (AMPH), the benzodiazepine anxiolytic chlordiazepoxide (CHDP), and the antidepressant desipramine (DMI) on DRL 72-s performance were evaluated using peak deviation analysis. The three compounds had distinctive effects on the peak-deviation-analysis metrics.

GENERAL METHOD

Overview of Peak Deviation Analysis

In the approach to IRT analysis described here, DRL IRT distributions are seen as reflecting relatively brief periods of interaction with the lever (bursting), during which one or more bar-press responses may occur. These periods of bar pressing are separated by long intervals (pausing). This burst/pause characterization of operant responding is not novel. A number of investigators have characterized responding on operant schedules in a similar fashion (Blough, 1963; Gilbert, 1958; Nevin & Baum, 1980; Pear & Rector, 1979; Premack, 1965; Shull, 1991; Wearden, 1983; Williams, 1968). On DRL schedules the presence of bursting is often obvious (see Figure 1A), and it is clear that combining short burst-IRT durations with longer pause-IRT durations will not usefully characterize the IRT distribution. In addition, on DRL schedules bursting is highly variable among rats (Richards & Seiden, 1991). Peak deviation analysis acknowledges the bimodal nature of many DRL IRT distributions by characterizing them as being made up of distinct burst and pause distributions. As was noted in the introduction, separate metrics are used to characterize the burst (BR) and pause (PkL, PkA) distributions.

For the purposes of peak deviation analysis, these two distributions are separated by a burst cutoff value. The resulting two IRT distributions are designated as the burst distribution (IRTs $<$ burst cutoff) and the pause distribution (IRTs $\geq$ burst cutoff). The burst cutoff value can be set at any value beginning with zero, which would indicate no burst cutoff. For the DRL 72-s schedule used in this paper, we have found that a burst cutoff value of 6 s works well (see Experiment 1). For example, the obtained relative frequency and CNE relative frequency histograms of a rat well trained on a DRL 72-s schedule of reinforcement are shown in Figure 1A. Inspection of Figure 1A shows that the bimodal shape of the obtained IRT distribution is markedly different from the CNE distribution. The first mode in the obtained IRT distribution (shaded bar on left) reflects a tendency of the sample rat to respond in bursts. The second mode (the shaded area on the right) indicates that the sample rat is systematically pausing between bar-press responses (or bursts of bar presses). Presumably, this second mode reflects the criterion IRT duration reinforced by the DRL 72-s schedule. As is typical of rats trained on the DRL 72-s schedule, the location of the second peak shows that the sample rat frequently does not wait long enough between bar-press responses to meet the 72-s criterion for reinforcement.

Peak deviation analysis characterizes bursting by determining the ratio of obtained IRTs in the burst category to the number of burst IRTs predicted to occur in the burst category by CNE. In Figure 1A the CNE was determined based on the mean of the pause IRTs with bursts (IRTs $<$ 6 s) excluded. The CNE was then extrapolated into the burst category (IRTs $<$ 6 s) to provide a prediction for the number of IRT durations expected to occur in the burst category if the rat emitted responses randomly at a constant overall rate with no difference between burst and pause responding. The burst ratio (BR) is the number of

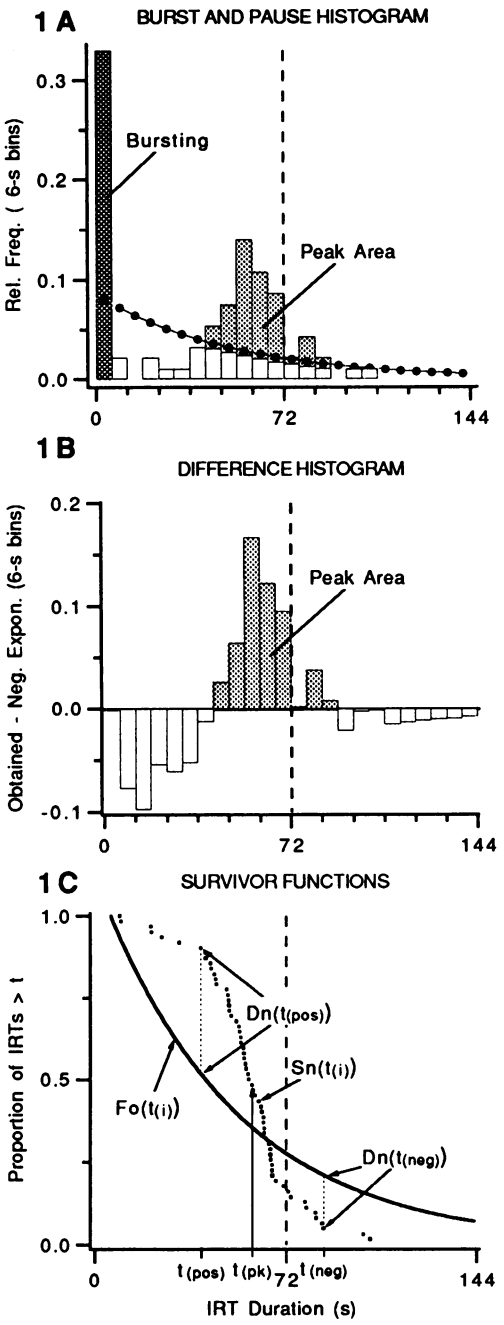

Fig. 1. The IRT distribution of a rat trained on a DRL 72-s schedule of reinforcement is plotted in three different ways in order to illustrate computation of the three peak-deviation-analysis metrics: peak area, peak location, and burst ratio. Plot 1A shows relative frequency histograms of the obtained (bars) and corresponding negative exponential (CNE) (connected dots) distributions. The CNE indicates the appearance of the IRT distribution if the rat emitted responses randomly in time with respect to the preceding response. The CNE is computed based on the pause IRTs with burst IRTs excluded. The single

obtained IRTs in the burst component divided by the number of IRTs predicted to occur in the burst component by the CNE. BR indicates the propensity to burst taking into account each rat's chance probability of bursting.

The pause distribution is characterized by determining the temporal location and area of the IRT durations that fall in the peak above the CNE (the shaded area in Figure 1A). This area can be further delineated by subtracting the CNE from the obtained IRT durations to form the difference histogram shown in Figure 1B. The shaded area above the zero line in Figure 1B corresponds to the shaded region in Figure 1A. The peak location (PkL) metric is the median IRT duration for the shaded region shown in Figure 1B. The peak area (PkA) metric is the area of the shaded region shown in Figure 1B. Computing relative frequency based only on the pause IRTs in Figure 1B insures that the total area under both the obtained pause and CNE distributions is always 1.0. This allows the pause distribution to be evaluated without being affected by the number of IRTs in the burst distribution.

A caveat about the distribution of burst responses needs to be made. Peak deviation analysis focuses on characterizing the distribution of pause responses. Although bursting is globally characterized with the burst ratio metric, the actual distribution of burst IRTs is not studied. The decision to focus on pausing resulted from two observations. First, the probability of occurrence of burst responding on

---

←

shaded histogram bar on the left indicates the burst component of the IRT distribution (IRTs < 6 s). The solid triangle within the shaded burst bar indicates the relative frequency of bursting predicted by extrapolation of the CNE into the burst category. The burst ratio (BR) measure is the ratio of the obtained to the predicted burst responses. The bars to the right of the burst component indicate the pause component of the IRT distribution (IRTs ≥ 6 s). Plot 1B shows a relative frequency difference histogram of the pause IRTs (IRTs ≥ 6 s). The difference histogram is computed by subtracting the CNE from the obtained pause IRT distribution. The difference histogram shows deviations from the CNE in 6-s bins. The peak area (PkA) is indicated by the shaded region of the obtained IRT histograms above the CNE in Plots 1A and 1B. The peak location (PkL) is the median IRT duration of the peak area. Plot 1C shows survivor plots of the obtained and CNE distributions. See text for explanation. The dashed vertical lines indicate the 72-s DRL criterion value.

DRL schedules is highly variable among rats. Some rats make few or no burst responses, whereas bursting accounts for more than half of the response output of other rats (see Richards & Seiden, 1991, p. 179, Table 1). The highly variable nature of bursting on DRL schedules makes systematic characterization of burst distributions difficult. In contrast, there is much less variability in the occurrence of pause responding among rats on DRL schedules. Second, previous observations have indicated that drugs have large, systematic effects on the pause component of DRL IRT distributions. This should not be construed as indicating that burst responding is unimportant. Detailed analysis of DRL burst distributions may also provide important information for the behavioral analysis of drug action.

Burst Responding

The burst ratio (BR) is the number of IRT durations in the burst category divided by the number of IRT durations predicted to occur in the burst category by the CNE. The BR is a standardized measure of the propensity of each rat to burst. Calculation of the expected number of burst-IRT durations is done by extrapolation of the CNE into the burst category.

As was developed in Richards and Seiden (1991), the number of IRTs predicted to fall between two time points $t1$ and $t2$ by the CNE is

$$(t1 < \text{IRT} < t2) = N(e^{-(t1-\text{cut})/(M-\text{cut})} - e^{-(t2-\text{cut})/(M-\text{cut})}),$$

where M is the mean of the pause IRT durations, N is the number of pause IRTs, and cut is the burst cutoff value. The value of BR then, can be calculated by dividing the number of IRTs in the burst category (Nb by the value obtained from the above equation with $t1 = 0$ and $t2 =$ cut. After setting $t1 = 0$ and $t2 =$ cut, the calculation of BR simplifies to

$$\text{BR} = Nb/[N(e^{\text{cut}/(M-\text{cut})} - 1)].$$

The BR metric is an attempt to compensate for differences in the probability of an IRT occurring in the burst category by chance alone. Measuring only the absolute or relative frequency of IRTs in the burst category ignores the fact that as the mean of the pause-IRT distribution becomes smaller, the chance probability of an IRT occurring in the burst category increases exponentially, not linearly. Consider two hypothetical IRT distributions, the first with a mean pause-IRT duration of 30 s with 60 IRTs in the burst distribution and 180 IRTs in the pause distribution, and the second with a mean pause-IRT duration of 60 s with 30 IRTs in the burst category and 90 IRTs in the pause category. For the first distribution, where the mean pause IRT is 30 s,

$$\text{BR} = 1.17 = 60/[180(e^{6/(30-6)} - 1)],$$

and for the second distribution, where the mean pause IRT duration is 60 s,

$$\text{BR} = 2.84 = 30/[90(e^{6/(60-6)} - 1)].$$

The BR value for the second distribution is greater despite the fact that it has fewer IRTs in the burst category and the relative frequencies of IRTs in the burst category are the same for the two hypothetical distributions.

Pause Responding

The histograms in Figures 1A and 1B serve to illustrate graphically the concepts behind the BR, PkA, and PkL measures using familiar graphical representations of the IRT distributions. However, construction of these histograms requires sorting the obtained IRT durations into intervals or bins. This sorting of the IRTs into class intervals (no matter what their size) results in a loss of precision, because the actual duration of each IRT is lost when it is accumulated into a class interval. In the present report, the approach described for calculating PkA and PkL does not involve sorting the IRTs into class intervals. Rather, the basis of this approach is the survivor curve illustrated in Figure 1C.

Survivor curves. The y axis of the survivor plot indicates the relative frequency (or proportion) of the pause IRTs with durations greater than or equal to the IRT duration indicated on the x axis. In other words, the y axis indicates the proportion of IRTs that "survived" to be greater than or equal to the duration indicated on the x axis. Figure 1C shows both the obtained and the CNE IRT distributions of the sample rat plotted as survivor curves. Each point of the obtained survivor curve represents an IRT duration emitted by the rat. As was the case for the difference histogram in Figure 1B, IRTs due to bursting (IRT < 6 s) have been excluded. The relative

survivor curve function, $Sn[t(i)]$, for the obtained pause IRTs is

$$Sn[t(i)] = i/N, \qquad i = 1, 2, 3, \ldots, N,$$

where $t(i)$ are the obtained IRT durations arranged in *descending* order and N is the total number of pause-IRT durations. It is important to note that $t(1)$ indicates the largest pause IRT duration and $t(N)$ indicates the smallest pause IRT duration. The CNE survivor function, $Fo[t(i)]$, is

$$Fo[t(i)] = e^{-(t(i)-\text{cut})/(M-\text{cut})}, \qquad i = 1, 2, 3, \ldots, N,$$

where M is the mean of the pause IRT durations, $t(i)$ indicates IRT duration, and cut is the burst cutoff value. The CNE survivor function predicts a corresponding value for each obtained $t(i)$. Subtracting the burst cutoff value (cut) from M and $t(i)$ adjusts the CNE survivor function so that $Fo[t(i)] = 1.0$ when $t(i) =$ cut because, by definition, all of the pause IRTs $\geq$ cut.

The absolute value of the slope at any point along the survivor curves indicates the relative frequency at which IRTs of the duration indicated on the x axis occurred. For example, the obtained survivor curve in Figure 1C is initially nearly flat and then drops steeply. The flat region indicates a relatively low probability of an IRT occurring. Conversely, the steep portion of the obtained survivor curve indicates a relatively high probability of an IRT occurring. There is a direct relationship between the relative frequency histogram plot in Figure 1A (excluding IRTs $<$ 6 s) and the survivor curves in Figure 1C. The absolute values of the slopes at any given point along the survivor curves in Figure 1C are proportional to the height of the histogram bars in Figure 1A. This means that the portion of the obtained survivor curve in Figure 1C that has the steepest slope corresponds to the shaded peaks in Figures 1A and 1B. The advantage of the survivor curve transformation over the IRT histogram transformation is that the duration of each IRT is represented and there is no loss of precision due to sorting of the IRT durations into class intervals.

To summarize, the ordinate of the survivor plot indicates the proportion of IRT durations that are longer than or equal to the duration indicated on the abscissa. The absolute value of the slope at any point along the survivor curve indicates the relative frequency of IRTs.

In order to calculate the PkA and PkL measures from the survivor function in Figure 1C, it is necessary to locate the segment of the obtained survivor curve that corresponds to the shaded portion of the histogram above the negative exponential indicated in Figures 1A and 1B. This portion of the survivor curve is designated as the peak segment. The peak segment of the obtained survivor curve is where IRTs occur more frequently than predicted by the CNE curve. In other words, the peak segment of the obtained survivor curve is the segment over which the slope of the obtained survivor curve is steeper than the slope of the CNE curve. Estimates of the end points of the peak segment can be readily obtained. One end of the peak segment is indicated by the IRT duration $t(\text{pos})$, where the difference ($Dn[t(\text{pos})]$) between the obtained and CNE survivor curves is greatest in the *positive* direction:

$$Dn[t(\text{pos})] = \max \{Sn[t(i)] - Fo[t(i)]\}, \qquad i = 1, 2, \ldots, N.$$

The other end of the peak segment is $t(\text{neg})$, where the difference ($Dn[t(\text{neg})]$) between the obtained and CNE survivor curves is greatest in the *negative* direction:

$$Dn[t(\text{neg})] = \min \{Sn[t(i)] - Fo[t(i)]\}, \qquad i = 1, 2, \ldots, N.$$

The end points of the peak segment obtained for the sample rat are indicated in Figure 1C.

To reiterate, $t(\text{pos})$ indicates the point at which the slope of the obtained survivor curve overtakes or becomes steeper than the slope of the CNE curve. $t(\text{neg})$ indicates the IRT duration at which the slope of the obtained survivor curve again becomes less than the slope of the CNE. Once $t(\text{pos})$ and $t(\text{neg})$ are located, the proportion of the obtained IRT durations (PkA) occurring within the peak segment that are not accounted for by the CNE can be calculated:

$$\text{PkA} = Dn[t(\text{pos})] + \text{abs}\{Dn[t(\text{neg})]\}.$$

The differences $Dn[t(\text{pos})]$ and $Dn[t(\text{neg})]$ are graphically illustrated in Figure 1C.

PkA has limits between 0.0 and 1.0. Because the obtained and CNE IRT distributions are converted to relative survivor curves, the largest possible value of PkA is 1.0. PkA = 1.0 will occur only if all of the obtained IRT durations have exactly the same value. The smallest possible value of PkA is 0.0. PkA =

0.0 indicates that the obtained distribution and the CNE distributions are identical.

PkL is the median of the IRTs located in the shaded peak segment above the CNE in Figures 1A and 1B. Given that PkA estimates the area under the peak with respect to the negative exponential, the IRT duration $t(i)$ in Figure 1C at which $Dn[t(\text{pos})] - Dn[t(i)]$ most closely approximates ½ of PkA estimates the median of the peak (Figure 1C):

$$\text{PkL} = \min\{\text{abs}[(Dn[t(\text{pos})] + \text{abs}(Dn[t(i)])) - .5\text{PkA}]\}, \quad i = \text{neg}, \text{neg} + 1, \ldots, \text{pos}.$$

As is indicated above, PkL is determined by searching between $t(\text{pos})$ and $t(\text{neg})$ for the obtained IRT duration $t(\text{pk})$ at which $Dn[t(\text{pos})] + \text{abs}\{Dn[t(i)]\}$ provides the closest approximation to ½ of PkA.

A step-by-step description of the peak deviation analysis procedure described above is provided in the Appendix.

EXPERIMENT 1

The basic idea of peak deviation analysis is to compare each rat's obtained IRT distribution to a corresponding negative exponential (CNE) distribution that predicts the appearance of the obtained IRT distributions had the rat emitted the same number of responses randomly in time. The CNE provides a standardized baseline for each subject, from which deviations can be measured. It is well known that rats trained on DRL schedules of reinforcement generate IRT distributions that have peaks reflecting the criterion IRT duration, as was shown for the sample rat in Figure 1A. These DRL IRT distributions do not resemble a negative exponential function. Because the DRL schedule enforces a contingency of reinforcement that specifies that only IRTs greater than a criterion duration will be reinforced, it is perhaps not surprising that DRL IRT distributions are not random (i.e., do not resemble the CNE distribution).

Although peak deviation analysis was designed to characterize DRL IRT distributions, this experiment examines IRT distributions produced by a contingency of reinforcement under which rats might be expected to perform more closely to the prediction of the CNE: a VI schedule. The contingency of reinforcement enforced by a VI schedule does not specify an IRT duration requirement for reinforcement (although in general longer IRT durations are more likely to be followed by reinforcement than are shorter IRT duration). Previous work (Anger, 1956; Kintsch, 1965) has shown that VI schedules, in contrast to DRL schedules, produce IRT distributions that are exponential in appearance.

The purpose of this experiment was to demonstrate how the metrics of peak deviation analysis characterize the differences between IRT distributions generated by training on VI and DRL schedules. This experiment compares DRL 72-s IRT distributions to IRT distributions generated by training on a VI 300-s schedule. The VI 300-s schedule was used because it provides a rate of reinforcement similar to that earned by rats on a DRL 72-s schedule. Extensive experience with the DRL 72-s schedule in this laboratory has shown that rats trained on this schedule average about 10 to 12 reinforcements per hour.

In this experiment, 6 rats were first trained on a VI 300-s schedule of reinforcement and were then trained on a DRL 72-s schedule of reinforcement. The resulting VI 300-s and DRL 72-s IRT distributions were then characterized using peak deviation analysis. The effect of varying the burst cutoff value on peak deviation analysis was examined.

METHOD

Subjects

Six male Sprague-Dawley rats (Holtzman, Madison, WI), weighing between 350 and 425 g, were used. The rats were housed 2 per cage in hanging stainless-steel wire cages. Lights were on in the colony room from 6 a.m. to 8 p.m. Food (4% Teklad rat chow) was available ad lib. Access to water was restricted to 20 min per day. On training days the rats received 20-min access to water at the end of their training session. On nontraining days (weekends), the rats were given 20-min access to water between 10 a.m. and 2 p.m.

Apparatus

Six operant conditioning chambers were used. Each chamber was 20.5 cm wide, 20.5 cm deep, and 23.5 cm long. The chambers had grid floors, aluminum front and back walls, and Plexiglas sides. A lever was mounted on the front wall 3 cm above the grid floor, 4.5 cm from the nearest side. A downward force of approximately 0.15 N was required for a

lever press to be detected. A solenoid-operated dipper (Gerbrands, Model G5600) was located 10 cm to the left of the lever. Access to the dipper was through a hole (4.5 cm diameter) in the front panel. Reinforcement consisted of lifting the dipper (0.025 mL) from a water trough to within reach of the rat's tongue for a period of 4 s. A stimulus light mounted 15 cm above the floor on the back wall of the chamber provided the only illumination. The stimulus light was turned on when a training session began and off when the training session ended. The chambers were enclosed in 80-quart Coleman® ice chests to attenuate external stimuli. Fans mounted on the ice chests provided ventilation and masking noise. The operant chambers were connected to a PDP-11/73® microcomputer via a Coulbourn Lablinc® interface. The schedule contingencies were programmed using the SKED-11® software system (Snapper, Stephens, Cobez, & Van Haaren, 1976). The timing resolution of the system was 0.01 s.

Procedure

Upon arrival in the colony, the rats were adapted to the water regimen (20 min per day access) for 1 week. The rats were then trained to bar press in five overnight training sessions using an alternative fixed-ratio (FR) 1 fixed-time (FT) 1-min schedule. Each night the rats were given four 30-min training sessions separated by 2-hr intervals. The duration of each session was signaled by turning the stimulus light on and off. At the end of this 5-day training period, all of the rats were lever pressing.

The schedule was then changed to a VI 300-s schedule of reinforcement. The rats were trained using 1-hr daily sessions, 5 days per week. The interreinforcement intervals for the VI 300-s schedule were generated using the progression described by Catania and Reynolds (1968). The intervals used were 25, 52, 82, 116, 153, 196, 246, 306, 381, 481, 631, and 931 s. The SKED-11 program that implemented the VI schedule sampled from the above list without replacement. The rats were trained on the VI 300-s schedule for 37 sessions.

After 37 sessions of training on the VI 300-s schedule, the schedule was changed to a DRL 72-s schedule. The rats were trained on the DRL 72-s schedule for an additional 85 sessions before the DRL 72-s data reported here were collected. Each DRL 72-s session was terminated by the first response after 60 min or after 65 min had elapsed.

Data Analysis

The VI 300-s and DRL 72-s data analyzed here were taken from the last three sessions of VI 300-s training and the last four sessions of the DRL 72-s training. The measures of performance were burst and pause responses per hour, reinforcements per hour, BR, PkA, and PkL. These measures were calculated for individual animals and are reported as an average of three sessions for the VI 300-s data and four sessions for the DRL 72-s data. The effects of VI 300-s and DRL 72-s training on IRT distributions were evaluated using the peak deviation analysis described above. The IRT data were analyzed with the burst cutoff value set to 0, 1, 2, 4, and 6 s for both the VI 300-s and DRL 72-s schedules. The Kolmogorov–Smirnov goodness of fit test was used to determine if each rat's obtained and CNE distributions were significantly different from each other (Gibbons, 1985).

For graphical presentation, the relative frequency histograms of individual-animal IRT distributions were averaged across the 6 rats. For an explanation of the relative frequency histograms, see the introduction and General Method section (Figures 1A and 1B).

Results and Discussion

VI 300-s Schedule

The effects of applying peak deviation analysis to VI 300-s IRT distributions with the burst cutoff set to 0, 1, 2, 4, and 6 s are shown in Figure 2. The single shaded histogram bar on the left side of the five large IRT histograms indicates the relative frequency of responses in the designated burst category. (In the top panel there is no shaded bar because the burst cutoff was set to zero.) The widths of the shaded burst bars reflect the duration of the burst category. The solid triangle within the shaded burst bar indicates the relative frequency of bursting predicted by extrapolation of the CNE into the burst category. Open histogram bars indicate obtained relative frequency IRT distributions for pause responses (IRTs $\geq$ the burst cutoff). All of the open histogram bars, including the first one after the burst category, are equal to 6 s. The connected solid dots show

the relative frequencies predicted to occur by the CNE for pause IRTs.

The difference histograms (insets) are computed by subtracting the CNE from the obtained pause IRT distribution. The difference histograms show deviations from the CNE in 6-s bins. Note that IRTs < the burst cutoff value are excluded from the difference histograms. The dashed vertical lines, which indicate 72 s, are included to facilitate comparison of the VI 300-s IRT distributions presented in Figure 2 with the DRL 72-s IRT distributions presented in Figure 3.

The tables adjacent to the histogram plots show individual-subject data. The column labeled Reinf indicates the number of reinforcers per hour obtained by each rat. The pause and burst columns indicate the number of pause and burst responses per hour emitted by each rat. The last three columns show the values of the peak deviation analysis metrics, BR, PkA, and PkL, for each rat. It should be noted that each time the burst cutoff was changed, the CNE was recalculated.

The difference between the CNE and the obtained IRT distribution was diminished as the value of the burst cutoff was increased for the VI 300-s schedule (see Figure 2, PkA values). The largest deviation from the CNE occurred at short IRT durations. When the burst cutoff was set to 0 s or 1 s, the difference histograms show large deviations from the CNE. In contrast, the difference histograms show smaller deviations from the CNE when the burst cutoff was greater than or equal to 2 s. Five of the rats had IRT distributions that were significantly different from the CNE, according to a Kolmogorov–Smirnov goodness of fit test, when the burst cutoff was set to 0 s (indicated by check marks on the right side of the data tables). In contrast, only 1 of the rats had an obtained IRT distribution that was significantly different from the CNE when the burst cutoff was greater than or equal to 4 s.

In addition to the graphical data of Figure 2, the PkA values demonstrate quantitatively that the difference between the predicted and obtained IRT distributions decreased as a function of burst cutoff. The PkA values for the individual subjects decreased as the value of the burst cutoff was increased, with the largest deviation from the CNE occurring at IRT durations less than 2 s. An interesting exception is Rat 523, which had a peak at longer IRT durations (13 to 18 s). In this rat, increasing the burst cutoff value did not decrease peak area. In addition, the Kolmogorov–Smirnov goodness of fit test indicates that the obtained IRT distribution of Rat 523 differed significantly from the CNE at all burst cutoff values.

For rats performing on a VI 300-s schedule, burst and pause responding are not described by a single negative exponential process. If the IRTs in the designated burst and pause categories were part of a single exponential distribution, then the CNE for the pause distribution (IRTs ≥ burst cutoff) should predict the number of IRTs in the burst category. The BR value is computed by dividing the obtained IRTs in the burst category by the expected number of IRTs in the burst category. A BR of 1.0 would indicate that the CNE correctly predicted the number of IRTs in the burst category. BR values were greater than one at all of the cutoff values tested. Only 1 rat (523) had a BR close to 1.0 (at 4-s and 6-s cutoff values), whereas the other rats had two to six times more burst IRTs than predicted by the CNE.

Summary. The VI 300-s IRT histogram plots in Figure 2, the PkA values, and the results of the Kolmogorov–Smirnov goodness of fit test all indicate that for burst cutoffs greater than 2 s, the pause distributions are similar to the CNE. Increasing the burst cutoff caused the pause distribution to become more similar to the CNE. However, because the proportion of burst responses remained greater than the value predicted by the CNE (indicated by BR values > 1.0), bust and pause responding on the VI 300-s schedule were not described by a single negative exponential process.

DRL 72-s Schedule

The effects of applying peak deviation analysis to the DRL 72-s data with the burst cutoff set to 0, 1, 2, 4, and 6 s are shown in Figure 3. The explanation of the plots and tables is the same as for Figure 2.

The difference between the CNE and the obtained IRT distributions was enhanced as the value of the burst cutoff was increased for the DRL 72-s schedule (see Figure 3, PkA values). The DRL 72-s IRT distributions show a marked deviation from the CNE in the pause component (IRTs ≥ 6 s). As burst cutoff was

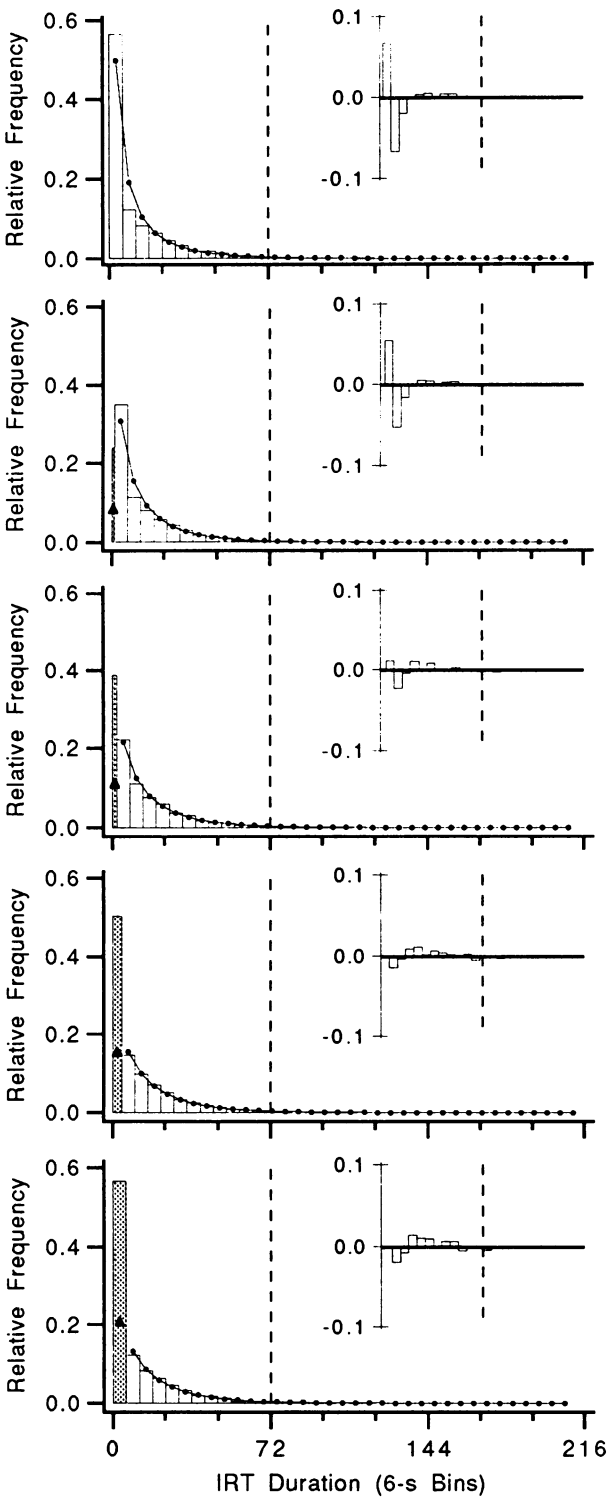

VI 300-s, Burst Cutoff = 0.0

ID	Reinf	Pause	Burst	BR	PkA	PkL
521	9.3	151.7	----	----	.17	1.3
522	10.3	754.0	----	----	.31	0.5√
523	11.3	272.7	----	----	.16	13.0√
524	11.3	1625.3	----	----	.20	0.4√
525	10.7	360.3	----	----	.20	0.9√
528	10.0	264.7	----	----	.22	1.4√
AVE	**10.5**	**571.4**	----	----	**.21**	**2.9**
SEM	0.3	227.2	----	----	.02	2.0

VI 300-s, Burst Cutoff = 1.0

521	9.3	139.3	12.3	2.18	.14	6.3
522	10.3	413.0	341.0	5.64	.17	1.4√
523	11.3	235.7	37.0	2.16	.17	17.6√
524	11.3	810.3	815.0	2.52	.16	1.5√
525	10.7	292.7	67.7	2.51	.12	1.3√
528	10.0	228.7	36.0	2.12	.19	1.8√
AVE	**10.5**	**353.3**	**218.2**	**2.85**	**.16**	**5.0**
SEM	0.3	98.5	129.4	0.56	.01	2.6

VI 300-s, Burst Cutoff = 2.0

521	9.3	123.0	28.7	3.07	.13	8.7
522	10.3	304.7	449.3	5.79	.12	3.0√
523	11.3	207.7	65.0	2.24	.20	17.4√
524	11.3	473.7	1151.7	3.59	.16	2.5√
525	10.7	238.0	122.3	3.05	.08	3.5
528	10.0	183.7	81.0	3.40	.16	22.4√
AVE	**10.5**	**255.1**	**316.3**	**3.52**	**.14**	**9.6**
SEM	0.3	50.1	178.4	0.49	.02	3.5

VI 300-s, Burst Cutoff = 4.0

521	9.3	109.7	42.0	2.55	.13	12.3
522	10.3	215.7	538.3	5.14	.08	4.8
523	11.3	189.0	83.7	1.42	.21	17.6√
524	11.3	218.7	1406.7	5.79	.08	6.1
525	10.7	194.3	166.0	2.48	.07	20.0
528	10.0	142.3	122.3	3.72	.18	33.2
AVE	**10.5**	**178.3**	**393.2**	**3.51**	**.12**	**15.7**
SEM	0.3	17.7	215.4	0.69	.02	4.3

VI 300-s, Burst Cutoff = 6.0

521	9.3	98.7	53.0	2.36	.11	11.8
522	10.3	164.3	589.7	4.95	.08	7.7
523	11.3	178.0	94.7	0.96	.18	17.8√
524	11.3	140.0	1485.3	6.08	.09	9.5
525	10.7	164.0	196.3	2.21	.07	15.1
528	10.0	126.7	138.0	3.13	.19	33.1
AVE	**10.5**	**145.3**	**426.2**	**3.28**	**.12**	**15.8**
SEM	0.3	12.0	226.1	0.78	.02	3.8

Fig. 2. IRT distributions of rats trained on VI 300-s schedules of reinforcement. The plots show the effects of setting the burst cutoff value to 0, 1, 2, 4, and 6 s. The IRT histogram plots represent the averaged relative frequencies of 6 rats. The tabular data to the right of each IRT histogram plot are for individual rats (see text). Training on the VI 300-s schedule produced IRT distributions that were similar to the CNE, particularly when IRTs < 4 s were excluded. Check marks on the right side of the tables indicate that the obtained IRT distribution was significantly

increased, this deviation was also increased. Note that this result is in direct contrast to that observed with the VI 300-s schedule.

The deviation of the obtained DRL 72-s IRT distribution from the CNE is described quantitatively by the individual-animal PkA values. The PkA values generated under the DRL contingency are larger than those generated under the VI contingency. Moving the burst cutoff from 0 s to 6 s increased the value of PkA for all 6 rats. The results of Kolmogorov–Smirnov goodness of fit tests indicate that the obtained DRL IRT distributions for each of the 6 rats were significantly different from the CNE at all five burst cutoff values.

Burst responding on the DRL 72-s schedule. The histogram plots in Figure 3 show that after training on the DRL 72-s schedule, the rats demonstrated a clear tendency to burst. This tendency is indicated by the relative frequency of IRTs in the burst categories and by the individual BR values shown in the tables. Most of the IRTs shorter than 6 s had durations under 2 s. As was previously described (Figure 2), most of the IRTs shorter than 6 s in the VI 300-s IRT distributions also had durations under 2 s. It is notable that despite the fact that the relative frequency of burst IRTs is greater in the VI IRT distributions (Figure 2) than in the DRL IRT distributions, the BR values for the DRL IRT distributions are at least as great as the BR values for the VI IRT distributions. These results indicate that the rats had a propensity to emit short IRT durations on both the VI 300-s and DRL 72-s schedules.

Choice of a 6-s Burst Cutoff Value

In the analysis of DRL 72-s schedule performance reported in Experiment 2 of this paper and in a previous study (Richards & Seiden, 1991), a 6-s burst cutoff value was used. As Figure 3 demonstrates, on DRL 72-s schedules, most of the IRTs that occur in the 0-s to 6-s burst category have durations of less than 2 s. The reason for using a longer bust cutoff of 6 s is to minimize the number of burst responses that are wrongly classified as pause responses. This approach, suggested by Slater and Lester (1980), helps to insure that the tendency to burst does not influence the analysis of the pause distribution. It probably should be noted that for DRL schedules with shorter duration IRT requirements, smaller burst cutoffs may be more appropriate. Another approach would be to use burst cutoffs adjusted for the IRT distributions of individual subjects. However, the experience of this laboratory has been that a uniform burst cutoff of 6 s works well for DRL 72-s schedules.

Comparison with Previous Reports

The PkL was shifted toward longer durations under the DRL contingency compared to the VI contingency. However the PkL generated by the DRL 72-s schedule was still less than the 72-s criterion. This result is consistent with previous studies (Richards & Seiden, 1991; see also Jasselette, Lejeune, & Wearden, 1990, and Zeiler, 1986, for reviews) that have also shown that animals trained on DRL schedules peak earlier than the criterion value, particularly at longer criterion values.

The shapes of the VI IRT distributions reported above are consistent with previous reports. Anger (1956) and Kintsch (1965) have reported IRT distributions for VI 300-s and VI 45-s schedules, respectively. Their plots had the same general shape as the VI IRT distributions presented here. In addition, using conditional probability plots (IRTs/OP), these authors graphically showed that short IRTs had the greatest conditional probability of occurring.

Summary of VI 300-s and DRL 72-s Schedule Comparisons

The primary goal of this experiment was to compare the IRT distributions of rats trained on VI 300-s and DRL 72-s schedules using

---

←

different from the CNE according to a Kolmogorov–Smirnov goodness of fit test. The large histograms show the obtained relative frequency (bars) and CNE (connected dots) IRT distributions. The CNE is computed with IRTs < the burst cutoff excluded. IRTs < the burst cutoff are indicated by the shaded histogram bars. The solid triangles within the shaded burst bars indicate the relative frequency of bursting predicted by extrapolation of the CNE into the burst category. The smaller histograms (insets) are relative frequency difference histograms for IRTs ≥ burst cutoff. The difference histograms are computed by subtracting the CNE from the obtained pause IRT distribution. The difference histograms show deviations from the CNE in 6-s bins. The dashed vertical lines that indicate 72 s are included in the VI 300-s plots to facilitate comparison with the DRL 72-s data presented in Figure 3.

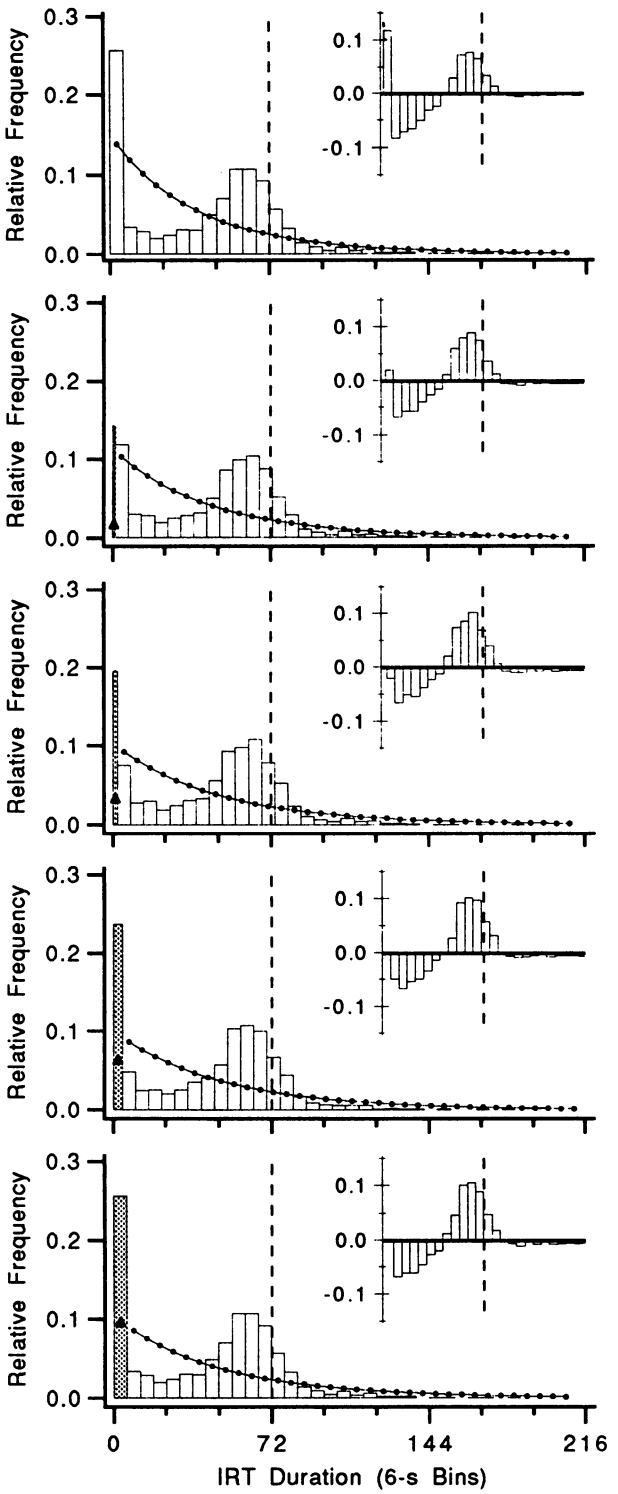

DRL 72-s, Burst Cutoff = 0.0

ID	Reinf	Pause	Burst	BR	PkA	PkL
521	9.5	69.0	----	----	.51	59.6
522	11.5	98.5	----	----	.35	34.6
523	8.8	90.3	----	----	.34	61.0
524	19.8	74.5	----	----	.35	67.2
525	9.0	105.3	----	----	.23	31.3
528	11.8	96.8	----	----	.39	48.4
AVE	**11.7**	**89.0**	**----**	**----**	**.36**	**50.3**
SEM	1.7	5.9	----	----	.04	6.1

DRL 72-s, Burst Cutoff = 1.0

521	9.5	63.3	5.8	4.98	.57	59.4
522	11.5	75.0	23.5	13.93	.41	65.5
523	8.8	84.5	5.8	2.62	.37	60.9
524	19.8	66.5	8.0	6.06	.40	67.0
525	9.0	93.5	11.8	4.64	.24	59.8
528	11.8	68.5	28.3	20.41	.51	63.7
AVE	**11.7**	**75.2**	**13.8**	**8.77**	**.42**	**62.7**
SEM	1.7	4.8	4.0	2.82	.05	1.3

DRL 72-s, Burst Cutoff = 2.0

521	9.5	62.5	6.5	2.80	.57	59.4
522	11.5	68.8	29.8	10.23	.45	65.5
523	8.8	78.8	11.5	2.92	.40	60.8
524	19.8	61.5	13.0	5.64	.44	66.8
525	9.0	85.5	19.8	4.48	.28	59.4
528	11.8	64.3	32.5	12.96	.55	63.7
AVE	**11.7**	**70.2**	**18.8**	**6.51**	**.45**	**62.6**
SEM	1.7	4.0	4.3	1.70	.04	1.3

DRL 72-s, Burst Cutoff = 4.0

521	9.5	61.5	7.5	1.58	.58	59.4
522	11.5	67.3	31.3	5.27	.45	65.5
523	8.8	74.3	16.0	2.16	.41	60.8
524	19.8	56.0	18.5	4.60	.50	66.7
525	9.0	76.3	29.0	3.83	.33	59.0
528	11.8	62.3	34.5	6.96	.56	63.7
AVE	**11.7**	**66.3**	**22.8**	**4.07**	**.47**	**62.5**
SEM	1.7	3.2	4.3	0.82	.04	1.3

DRL 72-s, Burst Cutoff = 6.0

521	9.5	60.8	8.3	1.12	.58	59.5
522	11.5	66.5	32.0	3.45	.45	65.5
523	8.8	70.0	20.3	1.94	.43	60.8
524	19.8	55.5	19.0	3.03	.50	66.7
525	9.0	72.3	33.0	3.02	.35	58.9
528	11.8	60.8	36.0	4.83	.57	63.7
AVE	**11.7**	**64.3**	**24.8**	**2.90**	**.48**	**62.5**
SEM	1.7	2.6	4.4	0.52	.04	1.3

Fig. 3. IRT distributions of rats trained on DRL 72-s schedules of reinforcement. The plots show the effects of setting the burst cutoff value to 0, 1, 2, 4, and 6 s. The IRT histograms represent the averaged relative frequencies of 6 rats. The tabular data to the right of each IRT histogram plot are for individual rats (see text). The plots show that training on the DRL 72-s schedule produced IRT distributions that were markedly different from the CNE. Kol-

peak deviation analysis. These two schedules provide similar overall rates of reinforcement but differ with respect to the degree of contingency between IRT duration and reinforcement. Examination of the individual-animal PkLs and PkAs in Figures 2 and 3 indicates that the obtained DRL 72-s pause distributions systematically deviated from the CNE. In contrast, the obtained VI 300-s pause distributions did not systematically deviate from the CNE. For the DRL 72-s schedule, the large deviation of the pause distribution from the CNE (indicated by the PkA values) shows that the pauses between bursts have durations that are controlled by the DRL 72-s schedule contingency. For the VI 300-s schedule, the similarity of the pause distribution (IRTs ≥ 6 s) to the CNE indicates that the pauses between bursts have durations that vary randomly. Taken together, these results demonstrate that PkA provides a measure of schedule control by the DRL contingency.

For the DRL schedule, unlike the VI schedule, no matter what burst cutoff value was used, the pause distribution remained different from the CNE. In fact, increasing the burst cutoff value increased the similarity between the predicted and obtained IRT distributions for the VI schedule and decreased the similarity between the predicted and obtained IRT distributions for the DRL schedule. This result suggests that both the VI and DRL IRT distributions were biased by the burst responses, albeit in opposite directions. Therefore, separating burst and pause responses allows the pause distribution to be analyzed without being biased by bursting, regardless of the schedule. For example, on the DRL 72-s schedule, when the burst cutoff was 0.0, the average PkA was 0.36 and the average PkL was 50.3. In contrast, when the burst cutoff was 6.0, the average PkA was 0.48 and the average PkL was 62.5 (Figure 3).

Training on both the VI 300-s and DRL 72-s schedules resulted in high probabilities for short-duration IRTs in comparison to the probability of pause responses, consistent with a burst/pause pattern of responding on both schedules. Examination of the individual-animal BR values suggests that burst responding was present in IRT distributions generated by both the DRL 72-s and VI 300-s schedules (although it must be conceded that the evidence for the burst/pause nature of VI 300-s performance is weaker). Given the presence of burst responding in both the VI 300-s and DRL 72-s schedules and the differences in degree of contingency between IRT duration and reinforcement, the results reported here suggest that the DRL IRT contingency asserts control over pause responding but not burst responding.

EXPERIMENT 2

In this experiment the effects of the psychomotor stimulant *d*-amphetamine (AMPH), the benzodiazepine anxiolytic chlordiazepoxide (CHDP),and the antidepressant desipramine (DMI) on DRL 72-s performance were compared.

The psychomotor stimulant AMPH has been shown to disrupt responding on DRL schedules of reinforcement. This disruption has been described as a leftward shift of the IRT distribution peak, accompanied by an increase in response rate (Segal, 1962; Sidman, 1955; Zimmerman & Schuster, 1962). Similarly, CHDP has been reported to increase response rate and shift the peak of the IRT distribution to the left on DRL schedules. However, AMPH and CHDP have been shown to have different effects on bursting. CHDP increases the proportion of burst responses, but AMPH does not (Sanger, 1980; Sanger & Blackman, 1975; Sanger, Key, & Blackman, 1974).

In contrast to AMPH and CHDP, the antidepressant DMI decreases response rate and increases reinforcement rate on DRL 18-s (McGuire & Seiden, 1980) and DRL 72-s

←

mogorov–Smirnov goodness of fit tests showed that obtained IRT distributions for each rat (at each of the five cutoff values) were significantly different from the CNE. The large histograms show the obtained relative frequency (bars) and CNE (connected dots) IRT distributions. The CNE is computed with IRTs < the burst cutoff excluded. IRTs < the burst cutoff are indicated by the shaded histogram bars. The solid triangles within the shaded burst bars indicate the relative frequency of bursting predicted by extrapolation of the CNE into the burst category. The smaller histograms (insets) are relative frequency difference histograms for IRTs ≥ burst cutoff. The difference histograms are computed by subtracting the CNE from the obtained pause IRT distribution. The difference histograms show deviations from the CNE in 6-s bins. The dashed vertical lines indicate 72 s.

(Seiden & O'Donnell, 1985) schedules of reinforcement. Inspection of IRT distributions indicates that the increase in reinforcement rate was accompanied by a systematic shift of the IRT distribution toward longer IRT durations. Importantly, the profiles of the IRT distributions did not appear to be changed by DMI, indicating that DMI did not disrupt responding as did AMPH and CHDP.

In the reports cited above, the assessments of drug effects on IRT distributions were based on qualitative descriptions of graphical presentations of the data. In the experiment below, we used peak deviation analysis to quantify these effects. By establishing quantifiable metrics that describe the IRT distribution, the effects of drugs (or other types of manipulation) on DRL IRT distributions can be standardized in the same way that response and reinforcement rates are standard measures, comparable across laboratories.

Method

Subjects, Apparatus, and Procedure

The rats and apparatus were the same as for Experiment 1. The doses of AMPH (*d*-amphetamine sulfate, Sigma) were vehicle, 0.50, 1.0, and 2.0 mg/kg. The doses of CHDP (chlordiazepoxide hydrochloride, Sigma) and DMI (desipramine hydrochloride, Sigma) were vehicle, 2.5, 5.0, 10.0, and 20.0 mg/kg. All drug doses were calculated as salts. CHDP and AMPH were dissolved in saline, and DMI was dissolved in water to form an injectable solution of 1 mL/kg. CHDP and AMPH were injected intraperitoneally 20 min prior to each session. DMI was injected intraperitoneally 1 hr prior to each session. The AMPH dose-response determination was completed during DRL 72-s Sessions 61 through 75. The CHDP dose-response determination was completed during DRL Sessions 96 through 110, and the DMI dose-response determination was completed during DRL 72-s Sessions 111 through 125. All three compounds were administered in ascending order twice a week on Tuesdays and Fridays.

Data Analysis

As in Experiment 1, burst and pause responses per hour, reinforcements per hour, and BR, PkA, and PkL measures were taken for each rat. The burst cutoff value was set to 6 s. When the number of pause IRTs (IRTs $\geq$ 6 s) in the pause distribution of an individual rat fell below 25, BR, PkA, and PkL were not computed.

In addition to presenting the data of individual rats at each drug dose, the group data were also analyzed for statistical significance across doses of the drug. This was done for burst responses, pause responses, reinforcements, BR, PkA, and PkL using a single-factor repeated measures analysis of variance. Because of the large variances for burst responding and the BR metric, a logarithmic transformation was applied to these data before statistical analysis (Winer, 1971, p. 400). If the overall F score was significant ($p < .05$), subsequent multiple comparisons were done using Duncan tests (Keppel, 1973). The repeated measures analysis of variance requires an equal number of subjects at each dose. Rat 521 failed to make at least 25 responses at the 20 mg/kg dose of CHDP, and Rat 523 failed to make at least 25 responses at the 20 mg/kg dose of DMI. The mean (BR, PkA, and PkL) values for the remaining 5 rats were substituted for Rats 521 and 523 at these doses in order to maintain an N of 6 in the statistical analysis.

Results

Amphetamine

The IRT plots in Figure 4 show the effects of the vehicle and the three doses of AMPH on the DRL 72-s IRT distributions. Tables adjacent to the IRT plots indicate individual-subject data as well as the mean and *SEM* at each dose of AMPH. AMPH significantly increased the rate of burst and pause responding at the doses tested. The rate of reinforcement was decreased. Figure 4 shows that the peak of the IRT distribution shifted toward shorter IRT durations as the dose of AMPH was increased. This effect is verified by the decrease in the PkL metric in all 6 rats. In addition, Figure 4 shows that the obtained pause-IRT distribution became increasingly similar to the CNE as the dose of AMPH increased. This effect is best demonstrated by the difference histograms in the figure insets. The effect was corroborated by a significant decrease in the PkA metric. Both the frequency and proportion of IRTs in the burst category were dose-dependently increased by AMPH. Despite this increase in the frequency and proportion of responses in the burst category, the BR metric

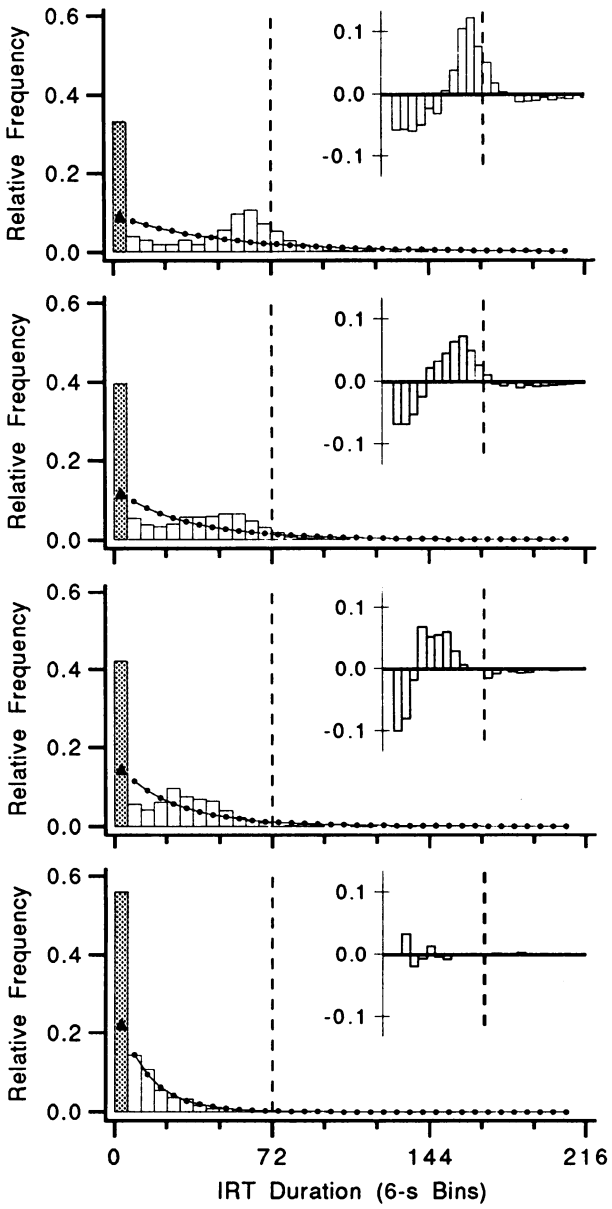

Veh. Amphetamine

ID	Reinf	Pause	Burst	BR	PkA	PkL
521	14.0	57.0	11.0	1.82	.62	60.8
522	11.0	71.0	50.0	4.79	.40	65.5
523	9.0	74.0	42.0	3.77	.36	60.6
524	9.0	75.0	45.0	3.80	.33	56.0
525	9.0	73.0	62.0	5.44	.39	56.3
528	18.0	54.0	16.0	2.85	.64	66.7
AVE	**11.7**	**67.3**	**37.7**	**3.74**	**.46**	**61.0**
SEM	1.5	3.8	8.2	0.53	.05	1.8

0.5 mg/kg Amphetamine

521	4.0	87.0	24.0	1.50	.44	40.4
522	1.0	130.0	164.0	3.72	.22	20.8
523	3.0	101.0	114.0	4.49	.21	49.6
524	4.0	90.0	64.0	3.52	.30	53.2
525	5.0	79.0	84.0	6.41	.43	50.7
528	11.0	60.0	10.0	1.42	.60	60.1
AVE	**4.7**	**91.2**	**76.7**	**3.51**	**.37**	**45.8**
SEM	1.4	9.6	23.4	0.77	.06	5.6
	*	*				*

1.0 mg/kg Amphetamine

521	3.0	101.0	52.0	2.24	.32	35.0
522	2.0	140.0	121.0	2.30	.11	20.3
523	4.0	114.0	122.0	3.67	.22	29.9
524	1.0	108.0	63.0	2.29	.48	29.9
525	2.0	89.0	98.0	5.54	.42	44.8
528	5.0	83.0	38.0	2.61	.41	42.3
AVE	**2.8**	**105.8**	**82.3**	**3.11**	**.33**	**33.7**
SEM	0.6	8.3	14.8	0.53	.06	3.7
	*	*	*		*	*

2.0 mg/kg Amphetamine

521	4.0	175.0	54.0	0.59	.18	11.5
522	2.0	197.0	203.0	1.42	.15	11.7
523	2.0	135.0	601.0	7.95	.07	15.8
524	4.0	159.0	359.0	3.97	.20	8.7
525	7.0	99.0	93.0	4.07	.20	26.1
528	2.0	151.0	247.0	3.54	.17	14.7
AVE	**3.5**	**152.7**	**259.5**	**3.59**	**.16**	**14.7**
SEM	0.8	13.8	81.6	1.05	.02	2.5
	*	*	*		*	*

Fig. 4. Effects of amphetamine on DRL 72-s performance. The plots show that amphetamine dose-dependently decreased peak area and shifted the peak location toward shorter IRT durations. The large histograms show the obtained relative frequency (bars) and CNE (connected dots) IRT distributions. The shaded histogram bars indicate bursting (IRTs < the burst cutoff). The solid triangles within the shaded burst bars indicate the relative frequency of bursting predicted by the CNE. The smaller histograms (insets) are relative frequency difference histograms for IRTs ≥ burst cutoff. The difference histograms are computed by subtracting the CNE from the obtained pause IRT distribution. The difference histograms show deviations from the CNE in 6-s bins. The dashed vertical lines indicate the 72-s DRL criterion value. The histograms represent the average data of 6 rats. The tables to the right of the IRT histograms present corresponding data for individual rats (see text). The burst response, pause response, and reinforcer columns indicate hourly rates. The asterisks indicate that the group means are statistically significantly different from vehicle ($p < .05$).

was not systematically changed as the dose of amphetamine increased.

Chlordiazepoxide

The IRT plots in Figure 5 show the effects of the vehicle and the four doses of CHDP on DRL 72-s IRT distributions. Tables adjacent to the IRT plots indicate individual-subject data as well as the mean and *SEM* at each dose of CHDP. Burst responding was increased in all 6 rats, but pause responding was not systematically affected. The number of reinforcers earned tended to increase, although this effect did not reach statistical significance.

The IRT histograms in Figure 5 indicate that the pause distribution became increasingly similar to the CNE as the dose of CHDP was increased. This effect was confirmed by a dose-dependent decrease in the value of PkA for all 6 rats. The modal IRT durations shifted toward shorter IRT durations as the dose of CHDP increased. There was a tendency for the PkL value to be decreased by CHDP. Examination of the individual-animal PkL values shows that this effect was not systematically observed in all rats. Because of the variability in this measure, the decrease was not statistically significant. The BR systematically increased as the dose of CHDP increased.

Desipramine

The IRT plots in Figure 6 show the effects of the vehicle and the four doses of DMI on DRL 72-s IRT distributions. Tables adjacent to the IRT plots indicate individual-subject data as well as the mean and *SEM* at each dose of DMI. Burst and pause responding were significantly decreased, and the number of reinforcers earned was significantly increased. The histograms in Figure 6 indicate that the profile of the IRT distribution was not changed by DMI. This effect was quantitatively confirmed by the fact that PkA was not significantly changed at any dose of DMI. Inspection of the IRT histograms also shows that the mode of the IRT distribution was shifted to the right. This effect was quantitatively confirmed by a statistically significant increase in the value of PkL. The BR was decreased by DMI.

Summary

In order to summarize the results of peak deviation analysis for AMPH, CHDP, and DMI, dose-effect curves for the three compounds are plotted side by side in Figure 7. The direction of change from baseline (if any) for mean response rate, BR, PkA, and PkL is shown in the table below the plots.

Total response rate was increased by AMPH and decreased by DMI (upper left panel of Figure 7). CHDP tended to increase total response rate, but this effect was not statistically significant. To allow direct comparison with previous reports, total response rate was defined as the total of both burst and pause responses per hour. Total response rate is simply the combined total of the burst and pause response columns of the tables in Figures 4, 5, and 6. BR was dose-dependently increased by CHDP. AMPH had no significant effect on BR, and DMI significantly decreased the value of BR (upper right panel of Figure 7). PkA was dose-dependently decreased by both AMPH and CHDP (lower left panel of Figure 7). In contrast, DMI did not significantly (statistically) change PkA at any of the doses tested. PkL was dose-dependently decreased by AMPH, whereas DMI had the opposite effect and dose-dependently increased the PkL value (lower right panel of Figure 7). CHDP tended to decrease PkL, but the effectiveness was not statistically significant.

Discussion

AMPH, CHDP, and DMI all affected the profile of DRL IRT distributions uniquely. The metrics of the peak deviation analysis quantitatively characterized these unique effects. The BR metric differentiated between the effects of AMPH and CHDP on burst responding. AMPH and CHDP increased both the absolute and relative frequency of burst responding (Figures 4 and 5), but only CHDP dose-dependently increased the value of BR.

Both AMPH and CHDP decreased PkA. In the case of AMPH, the decrease in PkA was accompanied by an increase in the rate of responding. In contrast, the decrease in PkA induced by CHDP was not accompanied by a statistically significant increase in the rate of responding, demonstrating that changes in PkA can occur independently of changes in total response rate. In contrast to AMPH and CHDP, DMI did not cause systematic changes in the PkA metric. The decrease in PkA induced by AMPH and CHDP indicates that these compounds caused the obtained IRT dis-

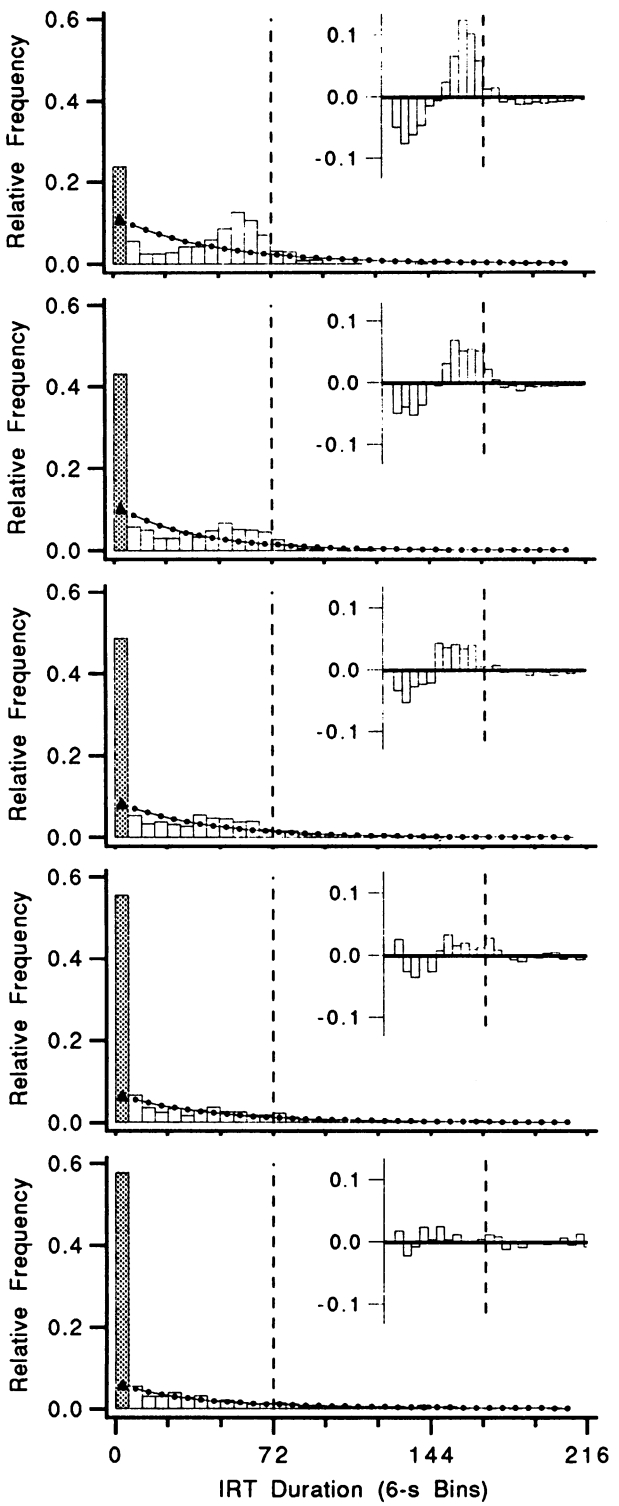

Veh. Chlordiazepoxide

ID	Reinf	Pause	Burst	BR	PkA	PkL
521	6.0	65.0	11.0	1.28	.56	57.4
522	8.0	77.0	42.0	3.36	.36	59.8
523	7.0	79.0	20.0	1.52	.39	61.2
524	9.0	70.0	32.0	3.12	.37	58.7
525	11.0	65.0	11.0	1.30	.44	53.5
528	9.0	64.0	24.0	2.92	.55	63.4
AVE	**8.3**	**70.0**	**23.3**	**2.25**	**.44**	**59.0**
SEM	0.7	2.7	5.0	0.40	.06	1.4

2.5 mg/kg Chlordiazepoxide

521	8.0	68.0	19.0	2.00	.48	60.3
522	14.0	65.0	68.0	8.04	.49	60.5
523	5.0	94.0	73.0	3.53	.22	59.8
524	3.0	110.0	96.0	3.24	.19	43.4
525	8.0	78.0	64.0	4.95	.29	50.2
528	7.0	82.0	85.0	5.86	.32	55.0
AVE	**7.5**	**82.8**	**67.5**	**4.60**	**.33**	**54.9**
SEM	1.5	6.9	10.8	0.88	.05	2.8
			*	*	*	

5.0 mg/kg Chlordiazepoxide

521	4.0	86.0	57.0	3.49	.42	42.3
522	14.0	75.0	127.0	10.52	.25	57.2
523	14.0	70.0	63.0	6.09	.17	61.7
524	14.0	62.0	33.0	4.21	.19	53.0
525	6.0	89.0	96.0	5.37	.23	45.5
528	15.0	68.0	87.0	8.94	.32	61.6
AVE	**11.2**	**75.0**	**77.2**	**6.44**	**.26**	**53.5**
SEM	2.0	4.3	13.5	1.1	.04	3.4
			*	*	*	

10 mg/kg Chlordiazepoxide

521	13.0	31.0	35.0	20.11	.20	53.7
522	4.0	108.0	290.0	9.73	.16	37.4
523	14.0	77.0	59.0	4.62	.19	58.8
524	16.0	51.0	68.0	13.29	.13	25.2
525	15.0	73.0	72.0	6.66	.19	46.5
528	17.0	76.0	101.0	7.99	.22	70.1
AVE	**13.2**	**69.3**	**104.2**	**10.40**	**.18**	**48.6**
SEM	1.9	10.7	38.2	2.28	.01	6.5
			*	*	*	

20.0 mg/kg Chlordiazepoxide

521	3.0	19.0	14.0	----	----	----
522	6.0	122.0	391.0	9.55	.09	8.6
523	11.0	55.0	70.0	11.46	.15	9.9
524	20.0	41.0	52.0	16.47	.13	126.3
525	4.0	98.0	150.0	6.65	.22	44.4
528	13.0	33.0	22.0	11.21	.25	49.7
AVE	**9.5**	**61.3**	**116.5**	**11.07**	**.17**	**47.8**
SEM	2.6	16.4	58.4	1.6	.03	21.4
			*	*	*	

Fig. 5. Effects of chlordiazepoxide on DRL 72-s performance. The plots show that chlordiazepoxide dose-dependently increased burst responding and decreased peak area. See Figure 4 for full description.

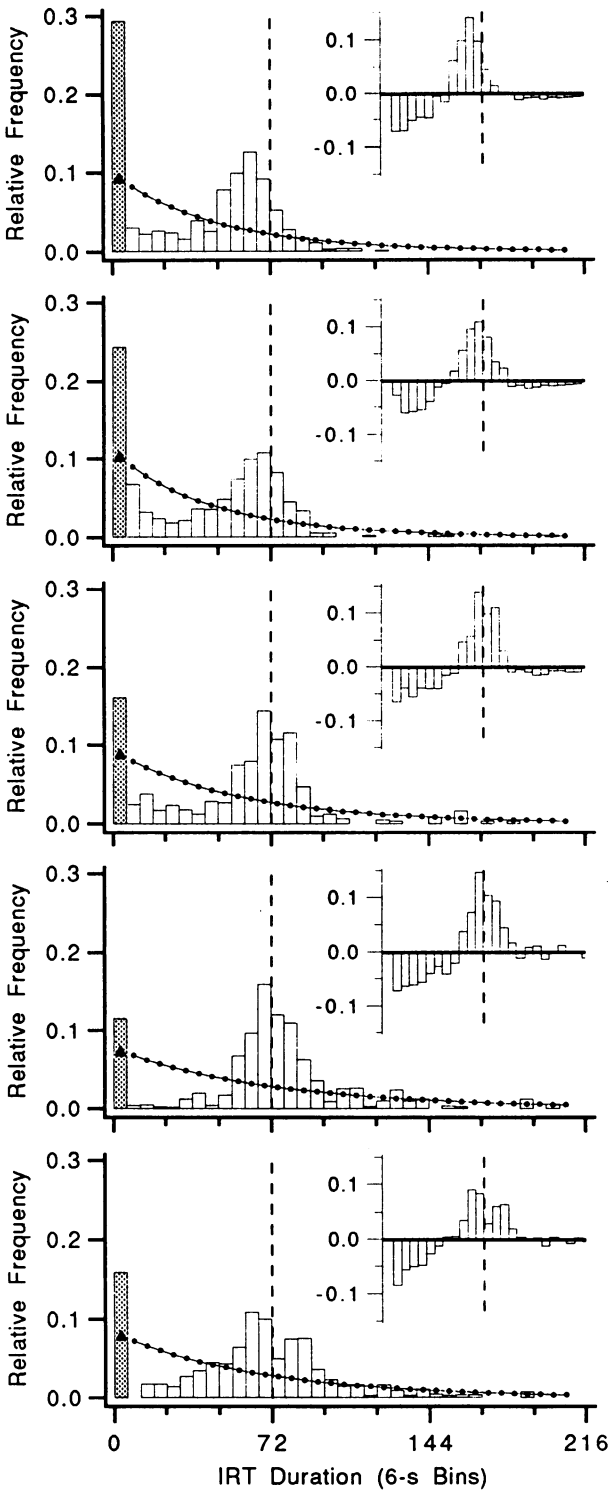

Veh. Desipramine

ID	Reinf	Pause	Burst	BR	PkA	PkL
521	7.0	59.0	9.0	1.29	.64	57.6
522	8.0	70.0	27.0	2.68	.42	65.1
523	11.0	72.0	29.0	2.65	.41	64.6
524	5.0	72.0	30.0	2.79	.49	55.4
525	15.0	59.0	53.0	7.62	.43	62.2
528	20.0	54.0	23.0	4.03	.63	67.8
AVE	**11.0**	**64.3**	**28.5**	**3.51**	**.50**	**62.1**
SEM	2.3	3.2	5.8	0.90	.04	2.0

2.5 mg/kg Desipramine

521	15.0	55.0	5.0	0.85	.64	69.3
522	2.0	96.0	58.0	2.81	.28	50.1
523	21.0	68.0	25.0	2.59	.32	73.1
524	14.0	63.0	17.0	2.11	.49	67.4
525	9.0	72.0	30.0	2.79	.39	59.7
528	23.0	51.0	15.0	2.96	.66	71.8
AVE	**14.0**	**67.5**	**25.0**	**2.35**	**.46**	**65.2**
SEM	3.2	6.5	7.5	0.32	.07	3.6

5.0 mg/kg Desipramine

521	22.0	46.0	2.0	0.48	.73	70.2
522	14.0	65.0	22.0	2.56	.43	68.0
523	25.0	38.0	3.0	1.13	.46	74.2
524	22.0	61.0	13.0	1.72	.45	71.0
525	14.0	66.0	31.0	3.46	.43	58.3
528	24.0	50.0	6.0	1.25	.70	71.7
AVE	**20.2**	**54.3**	**12.8**	**1.77**	**.53**	**68.9**
SEM	2.0	4.7	4.7	0.44	.06	2.3
	*		*	*		

10 mg/kg Desipramine

521	21.0	27.0	0.0	0.00	.50	105.3
522	24.0	49.0	5.0	1.07	.70	70.1
523	25.0	36.0	5.0	2.02	.59	75.4
524	22.0	48.0	8.0	1.79	.65	71.2
525	15.0	57.0	15.0	2.33	.55	66.5
528	28.0	48.0	7.0	1.60	.69	76.7
AVE	**22.5**	**44.2**	**6.7**	**1.47**	**.61**	**77.5**
SEM	1.8	4.4	2.0	0.34	.03	5.8
	*	*	*	*		*

20.0 mg/kg Desipramine

521	25.0	44.0	2.0	0.55	.48	78.5
522	24.0	43.0	10.0	2.85	.38	86.0
523	7.0	12.0	5.0	----	----	----
524	16.0	52.0	8.0	1.52	.67	64.2
525	20.0	54.0	15.0	2.62	.35	70.7
528	19.0	52.0	14.0	2.69	.42	65.0
AVE	**18.5**	**42.8**	**9.0**	**2.04**	**.46**	**72.9**
SEM	2.7	6.4	2.1	0.44	.06	4.2
	*	*	*	*		

Fig. 6. Effects of desipramine on DRL 72-s performance. The plots show that desipramine shifted the peak location toward longer IRT durations without disrupting the IRT distribution profile. See Figure 4 for full description.

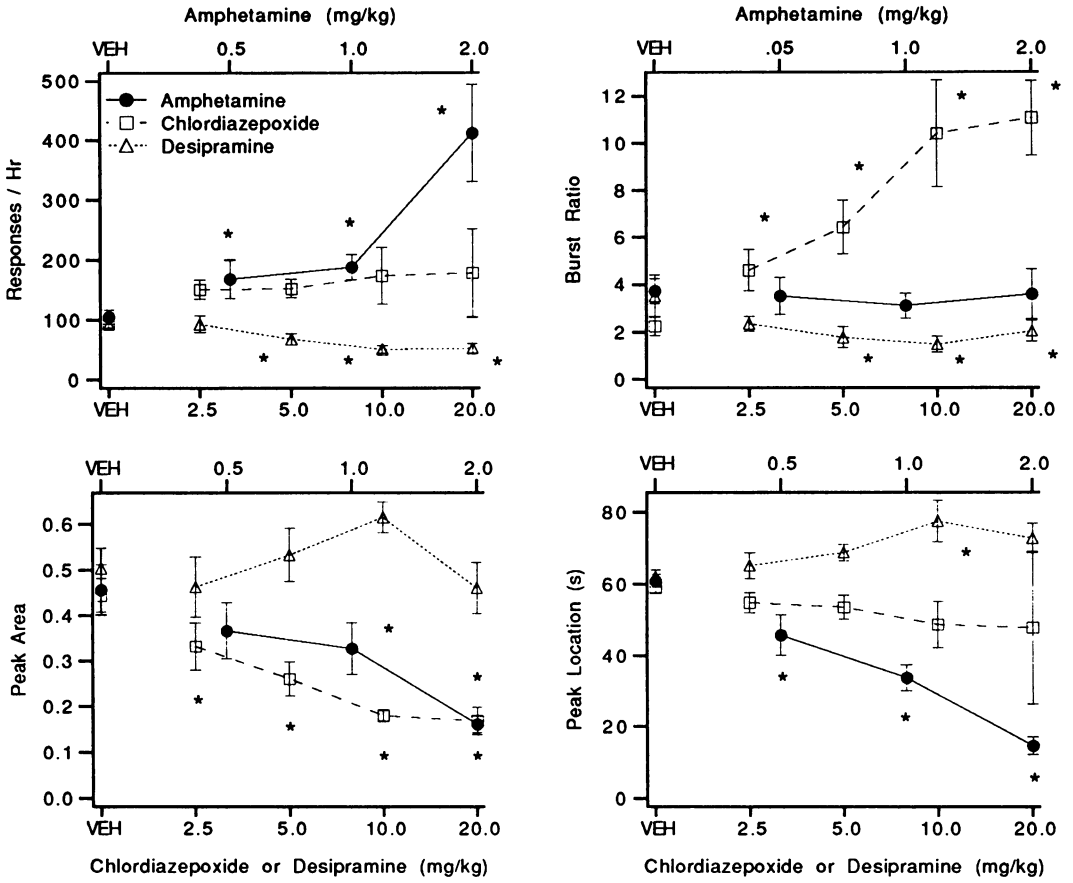

	Response Rate	Burst Ratio	Peak Area	Peak Location
Amphetamine	↑	—	↓	↓
Chlordiazepoxide	—	↑	↓	—
Desipramine	↓	↓	—	↑

Note: ↑ increase; ↓ decrease; — nochange

Fig. 7. Direct comparison of the dose-response determinations of amphetamine, chlordiazepoxide, and desipramine. Each of the three drugs had a unique pattern of effects as measured by response rate, burst ratio, peak area, and peak location. The table below the plots summarizes the drug effects by indicating the direction of drug-induced changes. The data are plotted as mean ± *SEM*. The asterisks indicate that the group means are statistically significantly different from vehicle ($p < .05$).

tribution to become similar to the CNE. In Experiment 1 it was suggested that PkA provides a measure of control over response output by the DRL 72-s IRT requirement. According to this interpretation, AMPH and CHDP, but not DMI, disrupted the control over response output by the DRL 72-s schedule.

The effects of AMPH, CHDP, and DMI on PkL reflected the effects of these compounds on total response rate. AMPH shifted PkL toward shorter IRT durations and increased total response rate. CHDP did not systematically change the PkL value and also did not significantly change total response rate. DMI

shifted PkL toward longer IRT durations and decreased total response rate. Decreases in total response rate, however, are not always associated with a shift in PkL toward longer IRT durations. For example, in a previous report (Richards & Seiden, 1991), we found that the serotonin 1A partial agonist gepirone decreased total response rate on a DRL 72-s schedule. The decrease in total response rate was accompanied by a decrease in PkA but no change in PkL.

The psychomotor stimulant AMPH shifted the PkL to the left, decreased PkA, and increased total response rate. Other psychomotor stimulants have been shown to have similar effects on DRL IRT distributions. For example, cocaine (Wenger & Wright, 1990), caffeine (Michaelis, Holloway, Bird, & Huerta, 1987), and methylphenidate (Seiden, Andresen, & MacPhail, 1979) have all been shown to increase total response rate and shift the mode of the DRL IRT distributions toward shorter IRT durations.

The benzodiazepine anxiolytic CHDP decreased PkA and increased the BR value. The effects of CHDP on BR are in agreement with previous reports indicating that a variety of anxiolytic compounds increase bursting on DRL schedules (see Sanger & Blackman, 1989, for a review). The decrease in PkA induced by CHDP is consistent with previous observations that CHDP disrupts the profile of DRL IRT distributions. Previously, this disruption has been described as a shift in the modal IRT duration toward shorter IRT durations (see Sanger et al., 1974, p. 165, Figure 5). In the present report CHDP also tended to shift the PkL toward shorter IRT durations. However, this effect was not systematic. In contrast, CHDP had large consistent effects on PkA. Examination of the PkA plots for AMPH and CHDP in Figure 7 shows that the effects of CHDP on PkA were equal to or greater than the effects of AMPH. However, AMPH had greater effects on PkL than did CHDP. The increased similarity of the obtained IRT distribution to the CNE induced by AMPH and CHDP indicates a loss of control by the 72-s IRT requirement for reinforcement. The differential effects of CHDP and AMPH on BR, total response rate, and PkL suggest that this loss of schedule control occurs through different mechanisms for the two drugs.

The antidepressant DMI shifted the peak of the IRT distribution toward longer IRT durations while decreasing BR and total response rate. In contrast to AMPH and CHDP, DMI did not decrease PkA. The effects of DMI in the present experiment are consistent with previous reports from this laboratory that have presented IRT histograms showing that antidepressant compounds shift the mode of the IRT distribution toward longer IRT durations without disrupting the profile of the IRT distribution (see Seiden & O'Donnell, 1985, for a review).

What emerges from the above description of drug effects is that AMPH, CHDP, and DMI all had unique profiles on DRL 72-s IRT distributions. The metrics of the peak deviation analysis quantitatively characterized these effects. This result suggests that drugs from different psychotherapeutic classes (i.e., psychomotor stimulants, benzodiazepine anxiolytics, and antidepressants) may have characteristic effects on DRL IRT distributions that can be used to differentiate these psychotherapeutic classes. Quantitative analysis of DRL schedule performance may therefore provide an effective behavioral assay system for identifying potential psychotherapeutic compounds and for studying the pharmacological effects of drugs on behavior.

GENERAL DISCUSSION

Behavioral Mechanisms Underlying Drug Effects

The DRL schedule contingency confronts the subject with a complicated task that can be disrupted in a variety of ways. Because of the complex nature of DRL performance, it is not appropriate to use a unitary behavioral mechanism (i.e., temporal discrimination) to explain the effects of drugs on DRL performance. Performance on this task not only involves time perception but also requires the animal to wait or inhibit responding in order to express a temporal discrimination. In addition, consider that DRL performance can also involve cognitive processes, such as reference and working memory. One view of DRL schedule performance (Meck, Church, & Olton, 1984) is that the subject must have a memory of the criterion value it was trained on (reference memory) as well as a memory of the elapsed time since the last response (working memory). Many other factors, such as sensory motor capability and reinforcing efficacy, can also affect DRL performance. The unique

effects of the three compounds tested here provide indirect support for the potential of DRL performance to be modified through more than one behavioral mechanism.

There are multiple behavioral mechanisms that may explain the drug effects observed in this experiment. For example, the shift in PkL toward shorter IRT durations caused by the psychomotor stimulant AMPH may be due to speeding up of an "internal clock" (Maricq, Roberts, & Church, 1981) or a decrease in the rat's ability to wait or inhibit response output (Robbins & Iversen, 1973). The decrease in PkA accompanying the shift in PkL toward shorter IRT durations supports the interpretation that the animal's ability to wait between responses is affected by AMPH. Conversely, the shift of PkL toward longer IRT durations caused by DMI may be due to a slowing of an internal clock or, alternatively, to an increase in the rat's ability to wait or inhibit response output (Bizot, Thiebot, Le Bihan, Soubrié, & Simon, 1988). The effect of CHDP on bursting is hard to account for. Bursting on DRL schedules may be due to a lack of feedback for unreinforced responses (Farmer & Schoenfeld, 1964; Fowler, 1980). Increases in bursting after administration of CHDP and other anxiolytics (Sanger & Blackman, 1989) may be due to a decrease in the animal's ability to detect stimuli normally associated with response completion.

It is clear that before an understanding of the behavioral mechanisms of drug effects on the DRL schedule can be successfully pursued, a better description of the behavioral mechanisms that underlie DRL performance is needed. Perhaps the quantitative IRT analysis described in this paper can provide a tool for studying more systematically the behavioral mechanisms involved in DRL performance. The unique effects of the three compounds tested and the potential for using the DRL schedule as part of a behavioral assay system accentuate the importance of understanding the behavioral mechanisms underlying DRL performance. Determining more precisely the behavioral mechanisms underlying DRL performance may provide greater insight into the behavioral actions of potential psychotherapeutic compounds. However, in the absence of a good understanding of the behavioral mechanisms involved in DRL performance, systematic changes in the IRT distribution profile can still be used to screen compounds. If it can be empirically shown that drugs from a particular pharmacological or psychotherapeutic class have a characteristic effect on DRL IRT distributions, then novel compounds that are found to have similar effect may also be of that particular drug class.

Quantitative IRT Analysis and the CNE

The results of both Experiments 1 and 2 show that under certain conditions the obtained pause IRT distributions resemble the CNE. In Experiment 1 rats were trained on a VI 300-s schedule that does not explicitly specify a temporal contingency between IRT duration and reinforcement. After training on the VI 300-s schedule, the pause-IRT distributions were found to be similar to the CNE. In addition, although the burst category appeared to be part of the same exponential function as the pause-IRT distribution, this was found not to be the case. The rats had more responses in the burst category than were predicted by the CNE. After specifying a strict temporal contingency between IRT duration and reinforcement by training the rats on a DRL 72-s schedule, the pause-IRT distributions developed peaks that deviated markedly from the CNE.

In Experiment 2 AMPH and CHDP changed the shape of the obtained pause IRT distributions, causing them to become more similar to the CNE. Experiment 2 demonstrates that disruption of the animal's ability to meet the temporal contingency enforced by the DRL schedule can result in responding in a random temporal fashion as described by the CNE. The results of both Experiments 1 and 2 add empirical validity to use of the CNE as a standard for characterizing the obtained IRT distribution. These results are consistent with the interpretation that decreases in PkA indicate loss of schedule control by the DRL contingency.

As was previously described in detail (Richards & Seiden, 1991, p. 185), the rationale behind the peak deviation analysis is similar to that of the IRTs-per-opportunity analysis of Anger (1956). The difference between the per-opportunity procedure and the present procedure is that peak deviation analysis uses the CNE curve to make a prediction about the opportunity or probability of an IRT of a given duration. In contrast, the per-opportunity procedure uses the frequency of IRTs equal to or greater than the target IRT duration to pro-

vide a prediction about the probability of an IRT of a given duration. Both procedures attempt to take into account the fact that by chance alone there is a higher probability of short IRTs occurring than long IRTs. The advantage of peak deviation analysis over the per-opportunity analysis is that it quantitatively characterizes the shape of the IRT distribution with the PkA and PkL metrics.

It is arguable that a simpler way to characterize DRL IRT distributions would be to compute the mean and standard deviation of the IRT distributions. Unfortunately, the bimodal nature of IRT distributions, due to bursting and also to the presence of very long IRT durations, limits the usefulness of mean and standard deviation for characterizing DRL IRT distributions. If outliers are eliminated, the mean and standard deviation may adequately characterize baseline DRL IRT distributions of well-trained animals. However, as was shown in this report for AMPH and CHDP and in a previous report (Richards & Seiden, 1991) for the serotonin 1A agonist gepirone, drugs often disrupt DRL IRT distributions, causing them to resemble a negative exponential distribution. As the DRL IRT distribution becomes increasingly more similar to a negative exponential distribution, the mean and standard deviation provide an increasingly less useful description of the IRT distribution. Peak deviation analysis, on the other hand, was designed to take into account the exponential character of DRL IRT distributions when the subject's ability to meet the temporal contingency is disrupted. The metrics of the peak deviation analysis measure deviations from the CNE, regardless of the kind of distribution (or distributions) that determine the peak.

Peak deviation analysis provides a way to characterize quantitatively the baseline performance as well as the effects of drugs. The metrics of the peak deviation analysis, in conjunction with response and reinforcement rate, provide a more precise characterization of DRL performance than do response and reinforcement rate alone. As was previously mentioned, similar response and reinforcement rates can be obtained from IRT distributions that have very different IRT distribution profiles. A more complete description of baseline performance using peak deviation analysis would insure that differences in obtained results (e.g., between laboratories) are not due to differences in baseline performance.

In conclusion, what we attempted to do with peak deviation analysis was to quantify the analysis of DRL IRT distributions in order to achieve standardization and greater sensitivity.

REFERENCES

Anger, D. (1956). The dependence of interresponse times upon the relative reinforcement of different interresponse times. *Journal of Experimental Psychology,* **52,** 145–161.

Bizot, J. C., Thiebot, M. H., Le Bihan, C., Soubrié, P., & Simon, P. (1988). Effects of imipramine-like drugs and serotonin uptake blockers on delay of reward in rats. Possible implication in the behavioral mechanism of action of antidepressants. *Journal of Pharmacology and Experimental Therapeutics,* **246,** 1144–1151.

Blough, D. S. (1963). Interresponse time as a function of continuous variables: A new method and some data. *Journal of the Experimental Analysis of Behavior,* **6,** 237–246.

Blough, D. S. (1966). The reinforcement of least-frequent interresponse times. *Journal of the Experimental Analysis of Behavior,* **9,** 581–591.

Catania, A. C., & Reynolds, G. S. (1968). A quantitative analysis of the responding maintained by interval schedules of reinforcement. *Journal of the Experimental Analysis of Behavior,* **11,** 327–383.

Duncan, I. J. H., Horne, A. R., Hughes, B. O., & Wood-Gush, D. G. M. (1970). The pattern of food intake in female brown leghorn fowls as recorded in a Skinner box. *Animal Behaviour,* **18,** 245–255.

Fagen, R. M., & Young, D. Y. (1978). Temporal patterns of behaviors: Durations, intervals, latencies, and sequences. In P. W. Colgan (Ed.), *Quantitative ethology* (pp. 79–114). New York: Wiley.

Farmer, J., & Schoenfeld, W. N. (1964). Effects of a DRL contingency added to a fixed-interval reinforcement schedule. *Journal of the Experimental Analysis of Behavior,* **7,** 391–399.

Fowler, S. C. (1980). Operant force emission during differential reinforcement of low rates. *Bulletin of the Psychonomic Society,* **15,** 251–253.

Gibbons, J. D. (1985). *Nonparametric methods for quantitative analysis* (2nd ed.). Columbus, OH: American Sciences Press.

Gilbert, T. F. (1958). Fundamental dimensional properties of the operant. *Psychological Review,* **65,** 272–282.

Jasselette, P., Lejeune, H., & Wearden, J. H. (1990). The perching response and the laws of animal timing. *Journal of Experimental Psychology: Animal Behavior Processes,* **16,** 150–161.

Keppel, G. (1973). *Design and analysis: A researcher's handbook.* Englewood Cliffs, NJ: Prentice-Hall.

Kintsch, W. (1965). Frequency distribution of interresponse times during VI and VR reinforcement. *Journal of the Experimental Analysis of Behavior,* **8,** 347–352.

Marek, G. J., Li, A. A., & Seiden, L. S. (1989). Evidence for involvement of 5-hydroxytryptamine$_1$ receptors in antidepressant-like drug effects on differential reinforcement-of-low-rate 72-second behavior. *Journal of Pharmacology and Experimental Therapeutics,* **250,** 60–71.

Maricq, A. V., Roberts, S., & Church, R. M. (1981). Methamphetamine and time estimation. *Journal of Experimental Psychology: Animal Behavior Processes,* **7,** 18–30.

McGuire, P. S., & Seiden, L. S. (1980). The effects of tricyclic antidepressants on performance under a differential-reinforcement-of-low-rates schedule in rats. *Journal of Pharmacology and Experimental Therapeutics,* **214,** 635–641.

Meck, W. H., Church, R. M., & Olton, D. S. (1984). Hippocampus, time, and memory. *Behavioral Neuroscience,* **98,** 3–22.

Michaelis, R. C., Holloway, F. A., Bird, D. C., & Huerta, P. L. (1987). Interactions between stimulants: Effects on DRL performance and lethality in rats. *Pharmacology Biochemistry and Behavior,* **27,** 299–306.

Mueller, C. G. (1950). Theoretical relationships among some measures of conditioning. *Proceedings of the National Academy of Sciences,* **36,** 123–130.

Nevin, J. A., & Baum, W. M. (1980). Feedback functions for variable-interval reinforcement. *Journal of the Experimental Analysis of Behavior,* **34,** 207–217.

Norman, M. F. (1966). An approach to free-responding on schedules that prescribe reinforcement probability as a function of interresponse time. *Journal of Mathematical Psychology,* **3,** 235–268.

O'Donnell, J. M., & Seiden, L. S. (1982). Effects of monoamine oxidase inhibitors on performance during differential reinforcement of low response rate. *Psychopharmacology,* **78,** 214–218.

Pear, J. J., & Rector, B. L. (1979). Constituents of response rate. *Journal of the Experimental Analysis of Behavior,* **32,** 341–362.

Premack, D. (1965). Reinforcement theory. In D. Levine (Ed.), *Nebraska symposium on motivation* (Vol. 13, pp. 123–180). Lincoln, NE: University of Nebraska Press.

Revusky, S. H. (1962). Mathematical analysis of the durations of reinforced interresponse times during variable interval reinforcement. *Psychometrika,* **27,** 307–314.

Richards, J. B., & Seiden, L. S. (1991). A quantitative interresponse-time analysis of DRL performance differentiates similar effects of the antidepressant desipramine and the novel anxiolytic gepirone. *Journal of the Experimental Analysis of Behavior,* **56,** 173–192.

Robbins, T. W., & Iversen, S. D. (1973). Amphetamine-induced disruption of temporal discrimination by response disinhibition. *Nature: New Biology* **245,** 191–192.

Sanger, D. J. (1980). The effects of caffeine on timing behaviour in rodents: Comparisons with chlordiazepoxide. *Psychopharmacology,* **68,** 305–309.

Sanger, D. J., & Blackman, D. E. (1975). The effects of tranquilizing drugs on timing behaviour in rats. *Psychopharmacologia,* **44,** 153–156.

Sanger, D. J., & Blackman, D. E. (1989). Operant behavior and the effects of centrally acting drugs. In A. A. Boulton, G. B. Baker, & A. J. Greenshaw (Eds.), *Neuromethods: Vol. 13. Psychopharmacology* (pp. 299–348). Clifton, NJ: Humana Press.

Sanger, D. J., Key, M., & Blackman, D. E. (1974). Differential effects of chlordiazepoxide and d-amphetamine on responding maintained by a DRL schedule of reinforcement. *Psychopharmacologia,* **38,** 159–171.

Segal, E. F. (1962). Effects of *dl*-amphetamine under concurrent VI DRL reinforcement. *Journal of the Experimental Analysis of Behavior,* **5,** 105–112.

Seiden, L. S., Andresen, J., & MacPhail, R. C. (1979). Methylphenidate and d-amphetamine: Effects and interactions with alphamethyltyrosine and tetrabenazine on DRL performance in rats. *Pharmacology Biochemistry and Behavior,* **10,** 577–584.

Seiden, L. S., Dahms, J. L., & Shaughnessy, R. A. (1985). Behavioral screen for antidepressants: The effects of drugs and electroconvulsive shock on performance under a differential-reinforcement-of-low-rate schedule. *Psychopharmacology,* **86,** 55–60.

Seiden, L. S., & O'Donnell, J. M. (1985). Effects of antidepressant drugs on DRL behavior. In L. S. Seiden & R. L. Balster (Eds.), *Neurology and neurobiology: Vol. 13. Behavioral pharmacology: The current status* (pp. 323–338). New York: Liss.

Shull, R. L. (1991). Mathematical description of operant behavior: An introduction. In I. H. Iversen & K. A. Lattal (Eds.), *Experimental analysis of behavior* (Part 2, pp. 243–282). Amsterdam: Elsevier.

Sidman, M. (1954). The temporal distribution of avoidance responses. *Journal of Comparative and Physiological Psychology,* **47,** 399–402.

Sidman, M. (1955). Technique for assessing the effects of drugs on timing behavior. *Science,* **122,** 925.

Slater, P. J. B., & Lester, N. P. (1980). Minimising errors in splitting behaviour into bouts. *Behavior,* **79,** 153–161.

Snapper, A. G., Stephens, K. R., Cobez, R. I., & Van Haaren, F. (1976). *The SKED software system: OS8 and time share SKED.* Kalamazoo, MI: State Systems.

Wearden, J. H. (1983). Undermatching and overmatching as deviations from the matching law. *Journal of the Experimental Analysis of Behavior,* **40,** 333–340.

Weiss, B. (1970). The fine structure of operant behavior during transition states. In W. N. Schoenfeld (Ed.), *The theory of reinforcement schedules* (pp. 277–311). New York: Appleton-Century-Crofts.

Wenger, G. R., & Wright, D. W. (1990). Behavioral effects of cocaine and its interaction with d-amphetamine and morphine in rats. *Pharmacology Biochemistry and Behavior,* **35,** 595–600.

Williams, D. R. (1968). The structure of response rate. *Journal of the Experimental Analysis of Behavior,* **11,** 251–258.

Winer, B. J. (1971). *Statistical principles in experimental design.* New York: McGraw-Hill.

Zeiler, M. D. (1986). Behavior units and optimality. In T. Thompson & M. D. Zeiler (Eds.), *Analysis and integration of behavioral units* (pp. 81–116). Hillsdale, NJ: Erlbaum.

Zimmerman, J., & Schuster, C. R. (1962). Spaced responding in multiple DRL schedules. *Journal of the Experimental Analysis of Behavior,* **5,** 497–504.

Received December 2, 1991
Final acceptance March 23, 1993

APPENDIX

Summary of Procedure

The following procedure was applied to the IRT distributions of individual subjects. A PASCAL program that implements the procedure described below is available from the authors upon request.

Step 1. The IRT durations were sorted into descending order and put into an array $t(i)$:

$$t(i), \qquad i = 1, 2, \ldots, \mathrm{J}.$$

$t(i)$ was the largest IRT duration and $t(J)$ was the smallest IRT duration, where J was the total number of IRT durations including both burst and pause IRTs.

Step 2. A burst cutoff value (cut) was defined. The smallest value of i at which $t(i) \geq$ cut was determined and called N. N was the number of IRT durations in the pause distribution. The number of IRT durations in the burst distribution was $Nb = J - N$. The mean of the pause distribution (M) was then calculated:

$$M = \left[\sum t(i)\right]/N, \qquad i = 1, 2, \ldots, N.$$

Step 3. BR was then calculated:

$$\mathrm{BR} = Nb/N(e^{\mathrm{cut}/(M-\mathrm{cut})} - 1).$$

Step 4. The sorted pause IRT durations were transformed into an obtained relative frequency survivor function $Sn[t(i)]$:

$$Sn[t(i)] = i/N, \qquad i = 1, 2, \ldots, N.$$

$Sn[t(i)]$ indicated the proportion of IRTs that were greater than or equal to $t(i)$.

Step 5. The corresponding negative exponential (CNE) survivor function $Fo[t(i)]$ was then calculated:

$$Fo[t(i)] = e^{-(t(i)-\mathrm{cut})/(M-\mathrm{cut})}, \qquad i = 1, 2, \ldots, N.$$

Step 6. A function $Dn[t(i)$ was generated according to the following algorithm:

for $i = 1, 2, \ldots, \mathrm{N}$
  if abs $\{Sn[t(i)] - Fo[t(i)]\}$
    $>$ abs $\{Sn[t(i)] - Fo[t(i-1)]\}$,
  then $Dn[t(i)] = Sn[t(i)] - Fo[t(i)]$,
  else $Dn[t(i)] = Sn[t(i)] - Fo[t(i-1)]$.

This algorithm computed differences between all of the obtained and predicted IRTs. It insured that the largest and smallest possible values of $Dn[t(i)]$ were generated. (For a further discussion of why both $Fo[t(i)]$ and $Fo[t(i-1)]$ were subtracted from each $Sn[t(i)]$ to determine the smallest and largest possible differences between the obtained IRT distributions and the CNEs see Gibbons, 1985, p. 63.)

Step 7. In order to calculate the PkA and PkL measures, the peak segment of the obtained survivor curve was demarcated. The value of i indicating the maximum *positive* deviation of the obtained survivor curve from the CNE survivor curve was located. This value of i was designed pos. t(pos) as the IRT duration at which $Dn[t(i)]$ had the maximum positive value:

$$Dn[t(\mathrm{pos})] = \max\{\mathrm{Dn}[t(i)]\}, \qquad i = 1, 2, \ldots, N.$$

The value of i indicating the maximum *negative* deviation of the obtained survivor curve from the CNE survivor curve was located. This value of i was designated neg. t(neg) was the IRT duration at which $Dn[t(i)]$ has the maximum negative value:

$$Dn[t(\mathrm{neg})] = \min\{Dn[t(i)]\}, \qquad i = 1, 2, \ldots, N.$$

The peak segment was $Sn[t(i)]$ between t(neg) and t(pos).

Step 8. The PkA was then computed:

$$\mathrm{PkA} = Dn[t(\mathrm{pos})] + \mathrm{abs}\{\mathrm{Dn}[t(\mathrm{neg})]\}.$$

Step 9. The peak location (PkL) is the IRT duration t(pk) between t(pos) and t(neg) at which

$$\mathrm{PkL} = \min[\mathrm{abs}\{Dn[t(\mathrm{pos})] - \mathrm{abs}(Dn[t(i)]) - 0.5\mathrm{PkA}\}], \qquad i = \mathrm{neg}, \mathrm{neg}+1, \ldots, \mathrm{pos}.$$

PkL was estimated by searching between t(pos) and t(neg) for the obtained IRT duration t(pk) that provided the closest approximation to ½ of PkA.

Multiple peaks. Sometimes, the pause IRT distributions being analyzed had more than one major peak. When this occurred, the largest peak was located and the peak segment was determined for that peak only. In order to take multimodal IRT distributions into account, the procedure described above was modified as follows. When t(neg) $>$ t(pos), the segment of the obtained survivor curve between t(pos) and t(neg) was steeper than the CNE. This result indicated that the peak segment had been cor-

rectly located. However if $t(\text{neg}) < t(\text{pos})$, the segment of the obtained survivor curve between $t(\text{pos})$ and $t(\text{neg})$ was flatter than the CNE.

This latter result indicated that the peak segment was not correctly located and that the IRT distribution being analyzed had more than one peak. Instead of identifying the major peak, the procedure had located the region between the two peaks. At this point, the procedure determined a peak segment for each of the two competing peaks. The procedure accomplished this by searching $Dn[t(i)]$ between $t(\text{neg})$ and $t(N)$ for the greatest value ($Dn[t(\text{pos}')]$) and between $t(1)$ and $t(\text{pos})$ for the smallest value ($Dn[t(\text{neg}')]$). The PkA between $t(\text{neg}')$ and $t(\text{pos})$ was then calculated, as was the PkA between $t(\text{neg})$ and $t(\text{pos}')$. The peak segment that had the largest PkA was used for the analysis.